3 3679 00054 1906

PNL-9819
UC-510

KINEMATIC ANALYSIS OF MODULAR, TRUSS-BASED MANIPULATOR UNITS

Robert James Salerno
Virginia Polytechnic Institute and State University
Blacksburg, Virginia

R. S. Stoughton, PNL Project Manager

June, 1994

Prepared for
the U.S. Department of Energy
under Contract DE-AC06-76RLO 1830

Pacific Northwest Laboratory
Richland, Washington 99352

Distribution

OFFSITE

2 DOE/Office of Scientific and Technical Information

Dr. William R. Hamel
Oak Ridge National Laboratory
Robotics and Process Systems Division
Oak Ridge, Tennessee 36831

ONSITE

DOE Richland Operations Office

Deborah Trader, K8-50

Westinghouse Hanford Company

William Joel Millsap, H5-68

11 Pacific Northwest Laboratory

Sharon Bailey
Carl Baker
Christina Mendoza
Bob Stoughton (2)
Publishing Coordination
Technical Report Files (5)

Summary

Decontamination and Dismantling (D&D) activities within the U.S. Department of Energy (DOE) require a long reach manipulator with a large load capacity. Variable Geometry Trusses (VGTs) are a unique class of mechanical structures which allow the advantages of truss structures for large scale applications to be applied to large robotic manipulators. Individual VGT units may be assembled to create a modular, long-reach, truss-type manipulator. Each module of such a manipulator system is either a static truss section or one of several possible VGT geometries. While many potential applications exist for this technology, the present work is largely motivated by the need for generic robotic systems for remote manipulation.

A manipulator system based on VGT modules provides several advantages. The reconfigurable nature of the manipulator system allows it to be adapted on site to unforeseen conditions. The kinematic redundancy of the manipulator enables it to work effectively even in a highly obstructed workspace. The parallel structure of the truss modules enables the manipulator to be withdrawn in the event of a structural failure. Finally, the open framework of the modules provides a clear, protected passageway for control and power cabling, waste conveyance, or other services required at the end effector.

As is implied in a truss structure, all primary members of a VGT are ideally loaded in pure tension or compression. This results in an extremely stiff and strong manipulator system with minimal overall weight. Careful design of the joints of a VGT is very important to the overall stiffness and accuracy of the structure, as several links (as many as six) are joined together at each joint.

The greatest disadvantage to this approach to manipulator design has traditionally been that the kinematics of VGT structures are complex and poorly understood. This report specifically addresses the kinematics of several possible geometries for the individual VGT units. Equations and solution techniques are developed for solving the "forward" or "direct" and "inverse" kinematic problems for these geometries. The "forward" kinematic problem is that of finding the position and orientation of the distal end of the VGT relative to the proximal end, given the specific displacements of the (linear) actuators. This problem is rarely solvable in closed form. However, powerful iterative algorithms capable of solution in real time on typical modern robot control hardware are presented. The "inverse" kinematic problem is that of finding the required actuator displacements given the position and orientation of the distal end of the VGT relative to the proximal end. For specific VGT geometries, closed-form solutions are presented. For the more general problem, iterative algorithms capable of solution in real time are again derived and presented.

Kinematic Analysis of Modular, Truss-Based Manipulator Units

Technical Report Prepared by

Robert James Salerno

Virginia Polytechnic Institute and State University

Prepared for Pacific Northwest Laboratories
January 1994

Abstract

Decontamination and Dismantling (D&D) activities within the U.S. Department of Energy (DOE) require a long reach manipulator with a large load capacity. This report discusses the kinematics of a new type of modular, long-reach, truss-type manipulator. Variable Geometry Trusses (VGTs) are used to construct a reconfigurable manipulator system in which all primary members are loaded in pure tension or compression. Each module of the manipulator system is either a static truss link or one of several possible VGT actuators, resulting in an extremely stiff and strong manipulator system with minimal overall weight. While many potential applications exist for this technology, the present work is largely motivated by the need for generic robotic systems for remote manipulation. This new manipulator system provides several advantages when used for this application. The reconfigurable nature of the proposed system allows the manipulator to be adapted on site to unforeseen conditions. Additionally, the kinematic redundancy of the manipulator ensures that solutions can be accomplished even in a highly obstructed workspace. The parallel structure of the truss modules enables the manipulator to be withdrawn in the event of a structural failure. Finally, of particular importance to these tasks, the open framework of the modules provides a passageway for waste conveyance, or can act as a shielded conduit for control and power cabling.

This work formalizes the concept of a canonical input specification set. The application of this concept results in greatly simplified analyses of many parallel manipulators. Although the manipulator system discussed was specifically developed for robotic handling of radioactive waste, the final resulting methodology is suited to a much broader class of problems - general underconstrained, redundant manipulator systems.

Contents

1 Introduction **1**
- 1.1 Background 1
- 1.2 The Proposed Manipulator System 1
  - 1.2.1 Overview of VGT Technology 3
  - 1.2.2 Benefits of Utilizing a Truss Structure 3
  - 1.2.3 Kinematic Complications 4
- 1.3 Outline of Contents 4

2 Literature Review **5**
- 2.1 Kinematics of Parallel Manipulators 5
- 2.2 Variable Geometry Truss Research 6
- 2.3 Redundant and Long-Reach Manipulator Research 7

3 Kinematics of Individual Truss Modules **9**
- 3.1 Truss Terminology and Notational Convention 10
- 3.2 Conventional vs. Canonical Input Specifications for the Forward Kinematic Analysis 13
- 3.3 Analysis of a Tetrahedral Module 17
  - 3.3.1 Forward and Inverse Kinematic Analysis 19
- 3.4 Analysis of a Longeron-Actuated, Octahedral Module 21
  - 3.4.1 Forward Kinematic Analysis 23
  - 3.4.2 Inverse Kinematic Analysis 28
- 3.5 Analysis of a General, Batten-Actuated, Double-Octahedral Module 29
  - 3.5.1 Forward Kinematic Analysis 31
  - 3.5.2 Inverse Kinematic Analysis 36
  - 3.5.3 Forward Kinematic Solutions with Symmetry Imposed . . . 37
  - 3.5.4 Inverse Kinematic Solutions with Symmetry Imposed 37
- 3.6 Description of the Static Truss Modules 41

4 Conclusion **43**

List of Figures

1.1 Typical Static and Active Truss Modules 2

3.1 Four Simple Spatial Unit Cells 11
3.2 A Typical Spatial Truss 12
3.3 Possible input specifications for a serial and parallel manipulator . . 14
3.4 Solutions for Alternative Input Specification Sets 15
3.5 Four Solutions to the Conventional Forward Kinematic Analysis of a Simple Parallel Manipulator. 16
3.6 Active Tetrahedral Truss Module 18
3.7 Schematic Tetrahedral Module with Analysis Parameters 20
3.8 General, Longeron-Actuated, VGT Module (A Stewart Platform) . 22
3.9 Kinematically Equivalent Devices Used for Analysis 24
3.10 Batten Actuated, Double-Octahedral VGT Module 30
3.11 Kinematic Equivalent to the Batten-Actuated, Double-Octahedral VGT 32
3.12 Method of projection through the plane of symmetry 38
3.13 Two Possible Goal Specifications for Closed-Form Inverse Analysis . 40
3.14 Possible Static Truss Sections 42

1. Introduction

This report focuses on the kinematic analysis of truss-based manipulators. Although this type of manipulator is applicable to many tasks, this work is motivated by the need to develop robotic systems for use in Decontamination and Dismantling (D&D) of contaminated facilities within the many U.S. Department of Energy (DOE) sites nationwide.

1.1 Background

The scheduled cleanup operations throughout DOE will require a rugged, reliable retrieval system sufficiently adaptive to the variety of waste types and equipment present. The physical requirements for accomplishing these tasks are demanding. The manipulator must be constructed to provide for a long reach, while maintaining the positioning accuracy of a payload as large as 2000 pounds [51].

1.2 The Proposed Manipulator System

A truss-based manipulator system (the proposed system) consists of relatively long, static links and compact, actuated joints. The major difference between the proposed system and conventional systems is the extensive use of truss technology. In terms of mechanical design, the joints for long-reach, large-load capacity manipulators present the single greatest difficulty in their construction, as these joints are subjected to enormous forces and torques while in service. Therefore, it is proposed that Variable Geometry Trusses (VGTs) be utilized to realize these joints. Hydraulically actuated VGT modules offer an ideal solution to the joint actuation problem posed by massive manipulators. In addition to utilizing VGTs for the joints, the links can also be constructed from truss elements. A typical pair of active and static modules is shown in Figure 1.1.

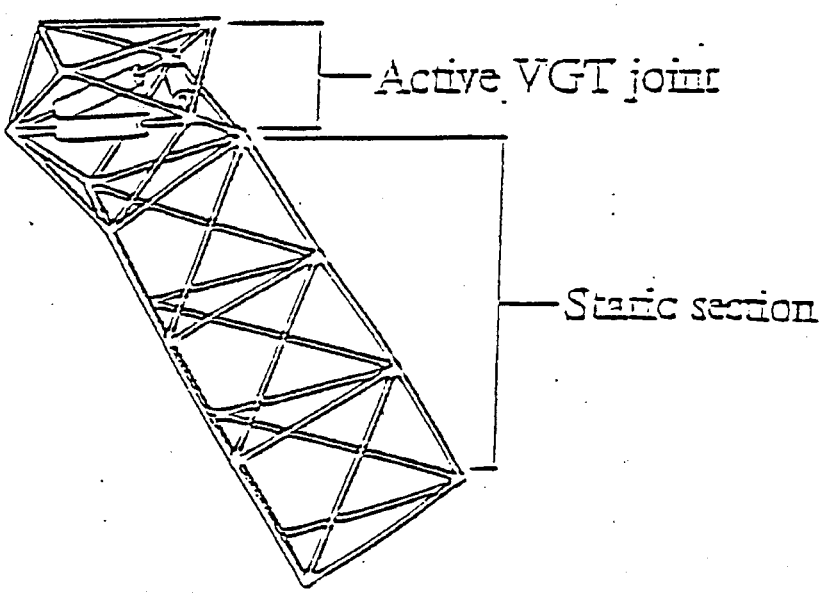

Figure 1.1: Typical Static and Active Truss Modules

1.2.1 Overview of VGT Technology

Robotic manipulators in use today are generally serially connected devices possessing six or fewer degrees of freedom. Purely serial manipulators are composed of a series of links connected to form an open chain. Each link of the manipulator is, in effect, a cantilever beam carrying the full load of all the links further out in the chain. The individual members of this chain may be subjected to all possible types of loads - bending, torsional, axial, and shear. The design is usually limited by the effects of torsional and bending loads. Consequently, most purely serial manipulators are inherently compliant and have relatively poor load-carrying capacities compared to their overall weight.

In contrast, parallel manipulators are composed of links connected to form one or several closed loops. A VGT manipulator is a special subset of parallel manipulators. Simply stated, an ideal VGT is a statically determinant truss that contains some number of variable-length members. These extensible members allow the truss to change shape in a precise, controllable manner. If properly designed, the primary members of a VGT manipulator will be predominantly loaded as two-force (pure tension/compression) members. There are negligible bending loads imposed by the mass of the individual links. This structural characteristic results in an extremely high stiffness-to-weight ratio, which enables some relatively light VGT manipulators to carry heavy payloads. These VGT modules are capable of supporting and manipulating several other modules, static or active, extended in a serial manner. Note that connecting these parallel structures in a serial manner imposes no bending or torsional loads on the individual truss members.

1.2.2 Benefits of Utilizing a Truss Structure

Most large-scale truss structures are composed of a repeating pattern of basic truss cells. This inherent modular structure has several advantages. It is possible to change the geometry of the manipulator by substituting different geometries of static or active modules, altering the order in which the modules are connected, or by changing the total number of modules present in the chain. In short, the manipulator may be reconfigured on site to adapt to unforeseen obstacles or other complications. Further, the modular structure ensures that damaged or worn components may be quickly exchanged to avoid a prolonged maintenance downtime.

The open framework of the truss structure is a great advantage over conventional manipulators. The open framework can be used for materials delivery, waste removal, or instrumentation and control cabling. Essentially, the exterior of the truss structure shields the more vulnerable components from abrasion and other hazards. The open framework allows the possibility of designing an integrated, internal waste conveyance system while still allowing easy access to the conveyance system. In this way, the conveyance system is not only protected, but does not restrict the manipulator's workspace in any way.

1.2.3 Kinematic Complications

There are disadvantages associated with the use of truss-type manipulators. The positional control strategies, which are relatively simple for conventional manipulators, become much more complicated. Not only are they complicated by the kinematic properties of the VGT modules, but also by the very general, modular nature of the system. If the manipulator is to be truly reconfigurable, there must be provisions for solving the kinematics of a new configuration without prior knowledge of how it will be assembled. The remainder of this report focuses on resolving the kinematic complications of the individual truss units.

1.3 Outline of Contents

Section 2 reviews the existing literature and appropriate background information. In Section 3, kinematic analyses of the individual modules is accomplished, with emphasis on the information required for conducting similar analyses on multi-module systems. Closed-form solutions are given for some truss geometries. For the remainder, computationally efficient iterative algorithms are presented.

2. Literature Review

The material presented within this report relies heavily on the fundamentals of kinematics, robotics, numerical analysis and geometric modeling. This literature review does not contain references to texts that contain these fundamental concepts. Instead, when appropriate, these texts will be referenced within the body of the report. This literature review presents publications that represent the past and current research on parallel, redundant and long-reach manipulators. To facilitate the organization of this material, the literature review is divided into three sections - kinematics of parallel manipulators, variable geometry truss research, and redundant and long-reach manipulator research.

2.1 Kinematics of Parallel Manipulators

Much of the early research conducted in robotics centered around the use of serially connected manipulators. Little attention was given to parallel manipulators until 1965, when Stewart [56] proposed the idea of a platform-type manipulator. This initial proposal showed that very rigid six degree-of-freedom (DOF) manipulators could be developed, but unfortunately, they had very restricted workspaces. Other than their practical implementation as flight and vehicle simulators, these devices remained somewhat of a novelty for many years. Perhaps one reason for this was the lack of adequate computing facilities to quickly solve the iterative kinematic constraint equations. The next decade witnessed tremendous advances in the field of robotics, but practically all the research was concerned solely with serial manipulators.

Further advances in parallel manipulators were put forth by Tesar and Cox [61] in 1981, Hunt [19] in 1983, Yang and Lee [65] in 1984, and Fichter [15] in 1985. Tesar and Cox performed the kinematic and dynamic analysis of a three DOF parallel manipulator. Hunt was concerned with the general analysis techniques for approaching the kinematics of parallel devices. Yang and Lee conducted a feasibility study on several geometrical variations of Stewart platforms. Fichter concentrated on the analysis and design of a Stewart platform based manipulator.

Research concerned with the dynamic analysis of parallel manipulators has been conducted by Sklar and Tesar [54] and Lee and Chao [25]. The work by Sklar and

Tesar was concerned with the dynamic analysis techniques for hybrid serial/parallel manipulators. This included several useful geometries for industrial manipulators. Lee and Chao focused on the kinematic and dynamic analysis of one particular geometry of a spatial three DOF manipulator. Sugimoto [58, 59] developed general computational methods for the dynamic analysis of parallel manipulators.

The papers cited above are all concerned with the analysis of parallel manipulators. Although none of these papers addresses the concept of a truss manipulator, many of the analysis techniques presented are applicable to VGTs.

2.2 Variable Geometry Truss Research

Simple VGTs are actually quite common and have been employed in engineering applications for decades. Many common configurations of construction cranes, draw-bridges, and similar devices can be classified as VGTs. However, most of these common applications utilize a VGT element as a single DOF mechanism. Stewart's early work, although technically not a truss structure, illustrated that it was possible to construct a fully parallel manipulator capable of positioning and orienting a platform in six dimensional space.

In the early eighties, the National Aeronautics and Space Administration (NASA) became interested in the development of "deployable" space structures [14]. NASA had many applications in space that required very large, stiff structures. A natural choice for such structures is a static truss. However, because of transport problems, these large structures must either be assembled in space or be transported in a compact form for later automatic deployment. Typically, these deployable structures become static once locked into their extended position.

While investigating possible geometries for these deployable structures, Rhodes and Mikulas [46] discovered that one certain geometry of deployable truss (a double-octahedral) had properties that made it suitable to act as a three DOF spatial manipulator. This was the first true VGT manipulator concept. Refinements were later made by Rhodes and Mikulas, in conjunction with Sincarsin [52], that led to the development of a working proof-of-concept model. This model not only solved many of the complex joint geometry problems, but also successfully demonstrated the potential usefulness of these devices. This insight made possible the work of Miura and Furuya [31], and Miura, et al. [30], who analyzed the kinematics of a double-octahedral VGT. This early analysis work was later extended by Gokhale and Reinholtz [45], and Padmanabhan, et al. [41]. The research of Padmanabhan is particularly interesting in that it identified several tasks for which a symmetric double-octahedral truss was well suited. This work then presents closed-form solutions to these tasks. Further refinements of the physical manipulator design were achieved by Tidwell, et al. in 1990 [62, 63]. This work included the development of design-curves that enabled quick evaluation of the potential motion of a double octahedral VGT.

Simultaneous with the development of the double-octahedral truss model, Sincarsin and Hughes [53] also explored the characteristics of four other candidate geometries. Their evaluations concluded that the double-octahedral geometry was indeed the most favorable geometry. Of primary interest in this study was the issue of collapsibility. Therefore, it should not be assumed that this is the best geometry for all applications. Jain and Kramer [20] also investigated another possible geometry and completed the design of a tetrahedral/tetrahedral VGT.

Other research concerning the use of a VGT cell as a replacement for more conventional devices has been conducted by Nayfeh [36], Clark and Robertshaw [10] and Wynn and Robertshaw [64]. Nayfeh investigated the kinematics of a foldable, revolute jointed space crane composed of several essentially planar VGT cells. The analysis undertaken was limited to only one of the proposed cells. Clark investigated the use of these VGT modules for actively damping vibration in large truss structures. This study dramatically illustrates the superiority of VGT actuators over conventional proof-mass type actuators for vibration control. This work was extended to the control of vibrations in spatial structures by Wynn in 1990. This last work included an impressive experimental demonstration of vibrations being actively controlled by a spatial VGT manipulator.

Natori, Iwasaki and Kuwao [35] have also investigated the vibration characteristics of long-chain planar trusses.

2.3 Redundant and Long-Reach Manipulator Research

Prior to 1988, interest in the concept of using VGTs for robotic manipulation remained somewhat limited. One primary reason for this lack of interest was the fact that these devices possessed relatively limited workspaces. This drawback can be overcome by joining several VGTs together end-to-end. This produces a long-chain manipulator whose workspace can be quite substantial . Miura, Furuya, and Suzuki [30, 31] were among the first to propose this long-chain structure in 1985. However, their solutions were limited by the assumption that all cells mimic the same motion. For their selected double-octahedral geometry, this constrained the motion of the manipulator to only three DOFs, regardless of the number of actuators present. This illustrates perhaps the second primary reason for the lack of interest in VGT manipulators. In short, these long-chain manipulators posed problems that were unheard of from the standpoint of conventional robotics. Most conventional manipulators are limited to six DOFs. Practical long-chain truss manipulators require from nine to sixty DOFs. No algorithms had yet been developed to satisfactorily solve the kinematics of these under-constrained systems. Shape control concepts provided a solution to this problem. These methods were introduced for planar VGT manipulators by Salerno and Reinholtz [49] in 1988, and were later refined to include an n DOF spatial manipulator system in 1989 [48, 50].

A simultaneous research effort, which yielded similar results, was accomplished by Chirikijan and Burdick [8, 9]. Naccarato and Hughes [33] have also developed similar algorithms. Of particular interest to the present application is the work done by Padmanabhan in 1989 [40]. This research addressed the design of a VGT-jointed, four DOF planar manipulator. The VGT joints replaced the revolute joints of a traditional manipulator structure. This work closely parallels the work presented here.

The concept of using curves or surfaces to determine the shape of a structure was briefly addressed by Natori, Iwasaki and Kuwao [35]. In their research, shape control concepts were utilized to yield an "adaptive planar truss structure" capable of forming a variety of parabolic shapes for large space antennae.

In recent years, much attention has been focused on redundant manipulators. As industrial manipulators find applications beyond the structured environment of the factory floor, redundancy provides these machines with the ability to adapt to unforeseen conditions. Many researchers [39, 22, 23] have sought methods that "resolve" the redundancy. Typically, these approaches sought to utilize the extra DOFs to control parameters other than the end-effector position. This is accomplished by adding constraints to the system until it is no longer under-constrained. Often, solutions can then be found in closed-form. An example of this is specifying not only an end-effector position but also an elbow position to ensure obstacle avoidance. Other approaches introduced kinetic constraints in addition to geometric constraints. Limiting or specifying characteristics of the joint velocities is an example of this method. Although these methods are appropriate to many situations, they eliminate many possible solutions in order to achieve fast processing times.

Another approach to resolving kinematic redundancy is to utilize the redundant DOFs to optimize some objective function. This is the approach used by Arnautovic [1], Mayorga and Wong [29], Suh and Hollerbach [60], and Carignan [6]. In this case, the necessary conditions of the optimization procedure provide the required constraints to identify a unique solution. The challenge to this task is identifying the optimum solution quickly.

Other related works of interest are Colbaugh and Jamshidi [11], Kelmar and Khosla [22], and Blume, et al. [5]. Colbaugh and Jamshidi specifically addressed the use of robotic manipulators for hazardous waste handling. Kelmar and Khosla proposed a fully serial, reconfigurable, modular manipulator system. Blume presented research on another large-scale manipulator system. This manipulator has a 22 meter reach and a 1.4 metric-ton payload.

3. Kinematics of Individual Truss Modules

To obtain a more detailed understanding of the complex motion characteristics associated with long-reach VGT manipulators, it is first necessary to gain a familiarity with the fundamental elements used in their construction. The science of kinematics provides a methodical way of analyzing the position, velocity, acceleration, and all higher-order derivatives of motion of these complex truss configurations. One definition of kinematics that is particularly appropriate to the study of VGT manipulators is as follows: *kinematics is the study of constrained motion of interconnected rigid links.* In this definition, the term *"rigid"* is used to describe the non-elastic behavior of the links and does not preclude the use of intentionally extensible links.

From a robotics viewpoint there are two distinct types of kinematic analyses: forward kinematic analysis and inverse kinematic analysis. Forward kinematic analysis (sometimes referred to as direct kinematic analysis) is concerned with finding the position and orientation of any or all members of a device, given only the geometric constraints of the individual links, the order and manner in which these links are assembled, and a set values for the control variables (typically either joint angles or extensible link lengths). Forward kinematic analysis could also be conducted to find the linear and angular velocities or accelerations of any member. This is often referred to as forward rate analysis, as opposed to forward position analysis.

Inverse kinematic analysis of a given device is concerned with finding a set control variable values that yields a desired position and/or orientation of a set of members. As a practical matter, in most useful devices, it is not possible to control the position and orientation of all members simultaneously. Again, the inverse rate analysis may be solved for any higher order derivative of motion, given a specified control variable input.

In the following sections, these concepts will be further developed for several different geometries of active truss modules. A comprehensive kinematic description of the static truss modules will also be developed.

3.1 Truss Terminology and Notational Convention

Many geometric configurations, both planar and spatial, are possible candidates for use as a VGT manipulator. This section will enumerate some of the possible geometries, introduce a convention for naming the links of a truss, and describe the notational conventions that will be used for analysis throughout this report.

The geometric structure on which all statically determinant planar trusses are based is the triangle. The triangle can therefore be thought of as the basic unit structure, or cell, used to construct all planar trusses. Spatial trusses present several possible cell structures that could be used to form a statically determinant truss. Four simple geometries are shown in Figure 3.1. The tetrahedron is the simplest geometry. More complicated geometries can be formed by connecting all vertices of a planar polygon to a pair of out-of-plane points, as illustrated in Figure 3.1. This type of geometric construction is referred to as di-pyramidal. Large-scale, statically determinant truss structures are commonly constructed with a replicating pattern of these basic unit cells.

A common static truss is shown in Figure 3.2. This truss is composed of three types of members. Those members that are oriented transverse to the truss axis are called battens. Those members that lie parallel to the truss axis are referred to as longerons. The remaining members, which lie neither parallel nor perpendicular to the truss axis, are identified as cross-longerons. In applying this nomenclature to variable-geometry trusses, it is often difficult, if not impossible, to distinguish between longerons and cross-longerons. For some geometries, a single member could fit both descriptions, depending on the length of the extensible members. For this reason, this report will refer to both groups simply as longerons. The points at which the truss members are joined will be called nodes.

To simplify notation, vectors expressed in a frame $\mathcal{F}$ will be identified by a leading-superscript $\mathcal{F}$ (for example, ${}^{\mathcal{F}}\vec{V}$). The length of fixed-length members will always be denoted by uppercase L's (for example L_3 or L_S). The length of all extensible members will be identified by lower case l's (for example l_3 or l_s). Some analyses may contain both L_3 and l_3. These lengths are not, in general, equal. Also, all position vectors will be described using spatial homogeneous coordinates and thus will be represented with 4×1 matrices.

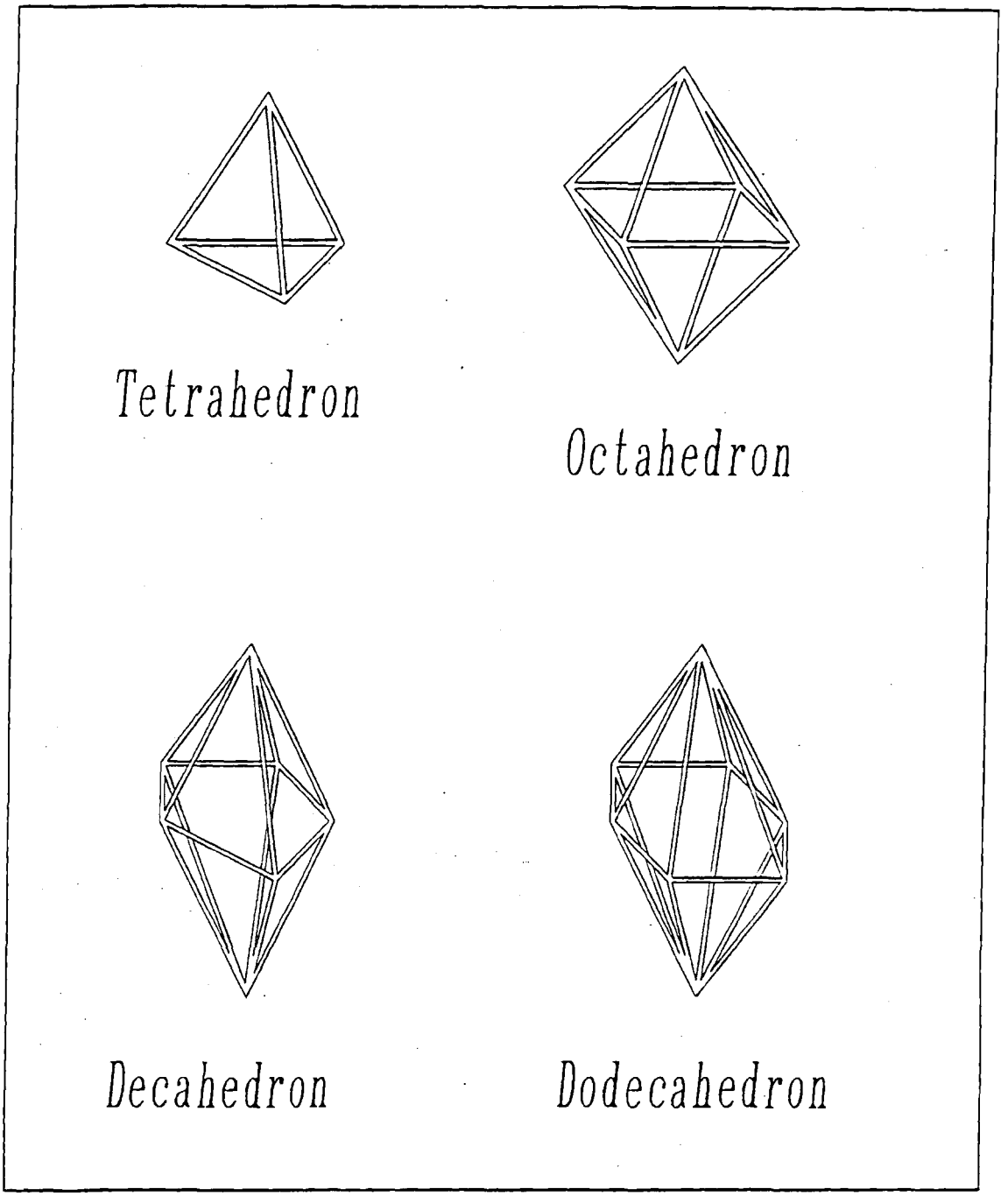

Figure 3.1: Four Simple Spatial Unit Cells

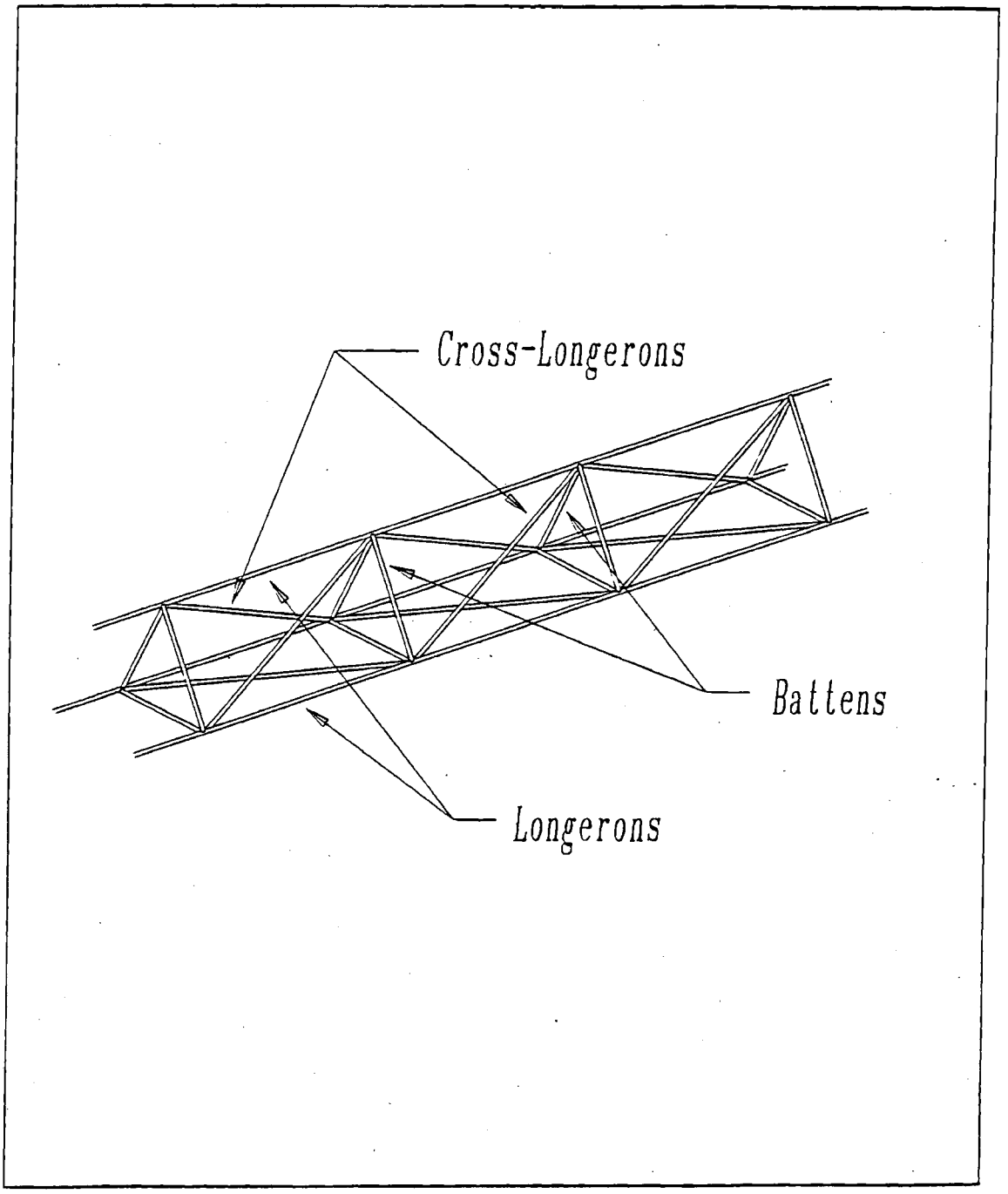

Figure 3.2: A Typical Spatial Truss

3.2 Conventional vs. Canonical Input Specifications for the Forward Kinematic Analysis

The goal of kinematic analysis, in general, is to develop motion input/output relationships for the devices studied. In the case of forward kinematics, the goal is to determine the system output given the system input. In terms of conventional forward kinematic analysis, the *input* is almost always interpreted as those parameters that are directly controlled. In other words, the same parameters that are adjusted by the physical actuators and measured by the instrumentation system. For most manipulators these inputs are either angular motions of a revolute joint or linear displacements of a prismatic joint. These seem to be natural parameters to specify as the input to the forward kinematics. These are, however, not the only possible input parameters. Some input specifications will be more convenient than others. The following simple examples will show that for some parallel manipulators these conventional input specifications may not necessarily be the most appropriate.

First, it must be understood that any set of independent parameters could be considered an input specification set, provided that the chosen parameters, when fixed, completely define the positional *state* of the manipulator - meaning that no further motion of the manipulator is possible. This does not mean that only one possible position of the manipulator exists for the given values. It is possible that other branches may satisfy the specified values. Naturally, an n degree-of-freedom device will require that n parameters be specified.

As an example, consider the simple planar two-link serial manipulator shown in Figure 3.3-A. It is easy to see how the two joint angles θ_1 and θ_2 could be used to control the XY position of point P. The conventional input specification would be θ_1 and θ_2. If θ_1 and θ_2 are fixed, no motion is possible. Also note that, the set of θ_1 and θ_2 has the property that it uniquely defines the position of the manipulator. This uniqueness is desirable, since it dictates that the solution will be closed-form and linear. Other valid specification sets are d and ψ, or the X coordinate of point A and θ_2. Although valid, neither is desirable because they do not uniquely define the position of the manipulator. Both result in two solutions to the forward kinematics. These solutions are depicted in Figure 3.4. Since no single unique solution results, the forward solution will be non-linear.

For most serial manipulators the conventional input specification set is the simplest, or canonical, input specification set.

Now, contrast these results with those of the parallel manipulator shown in Figure 3.3-B. It is easy to verify that the XY position of point P can be controlled, within a limited workspace, by changing l_1 and l_2. If the conventional input parameters, l_1 and l_2, are utilized, there are four solutions to the forward kinematics. These are illustrated in Figure 3.5. For this parallel manipulator, the conventional

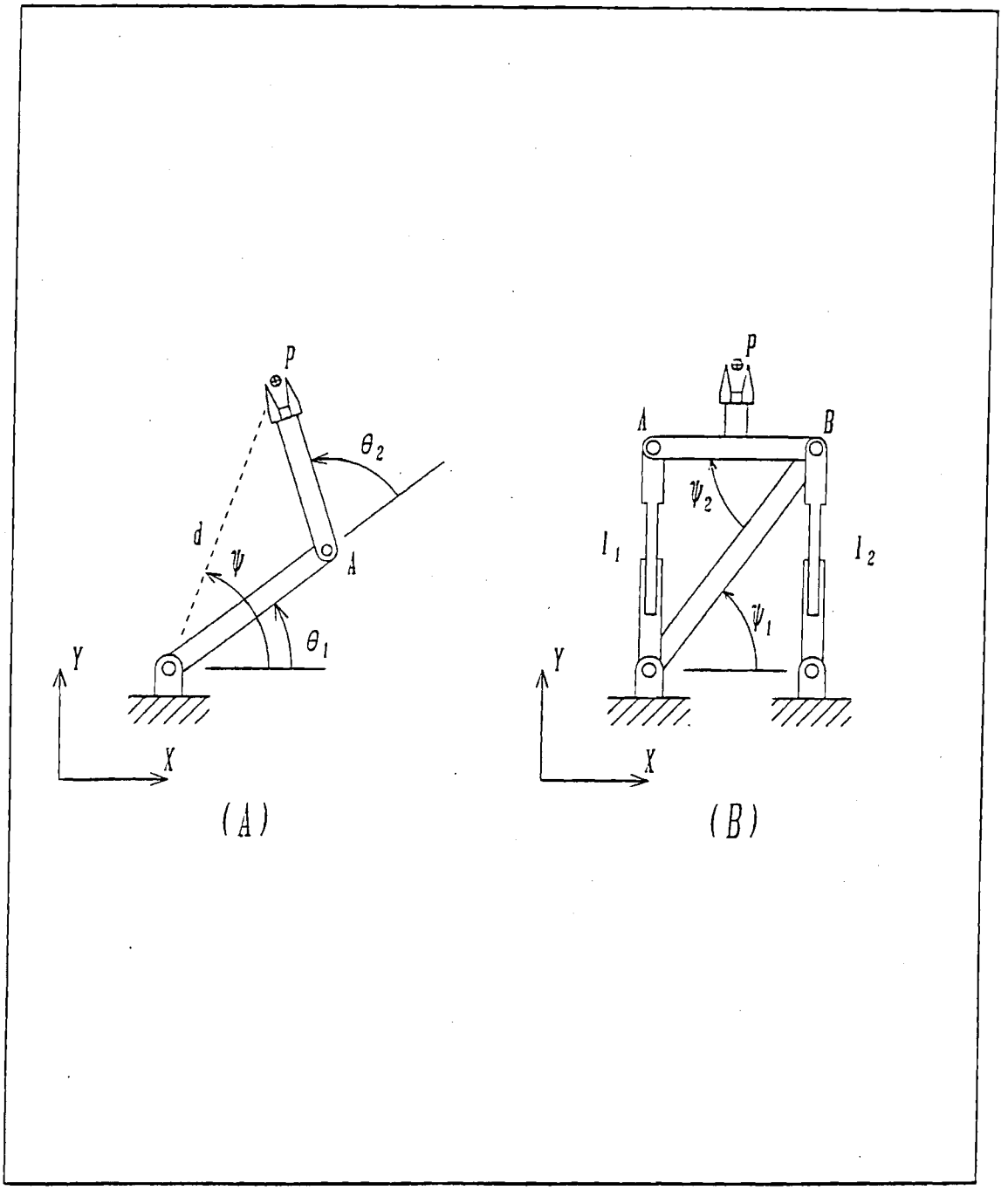

Figure 3.3: Possible input specifications for a serial and parallel manipulator

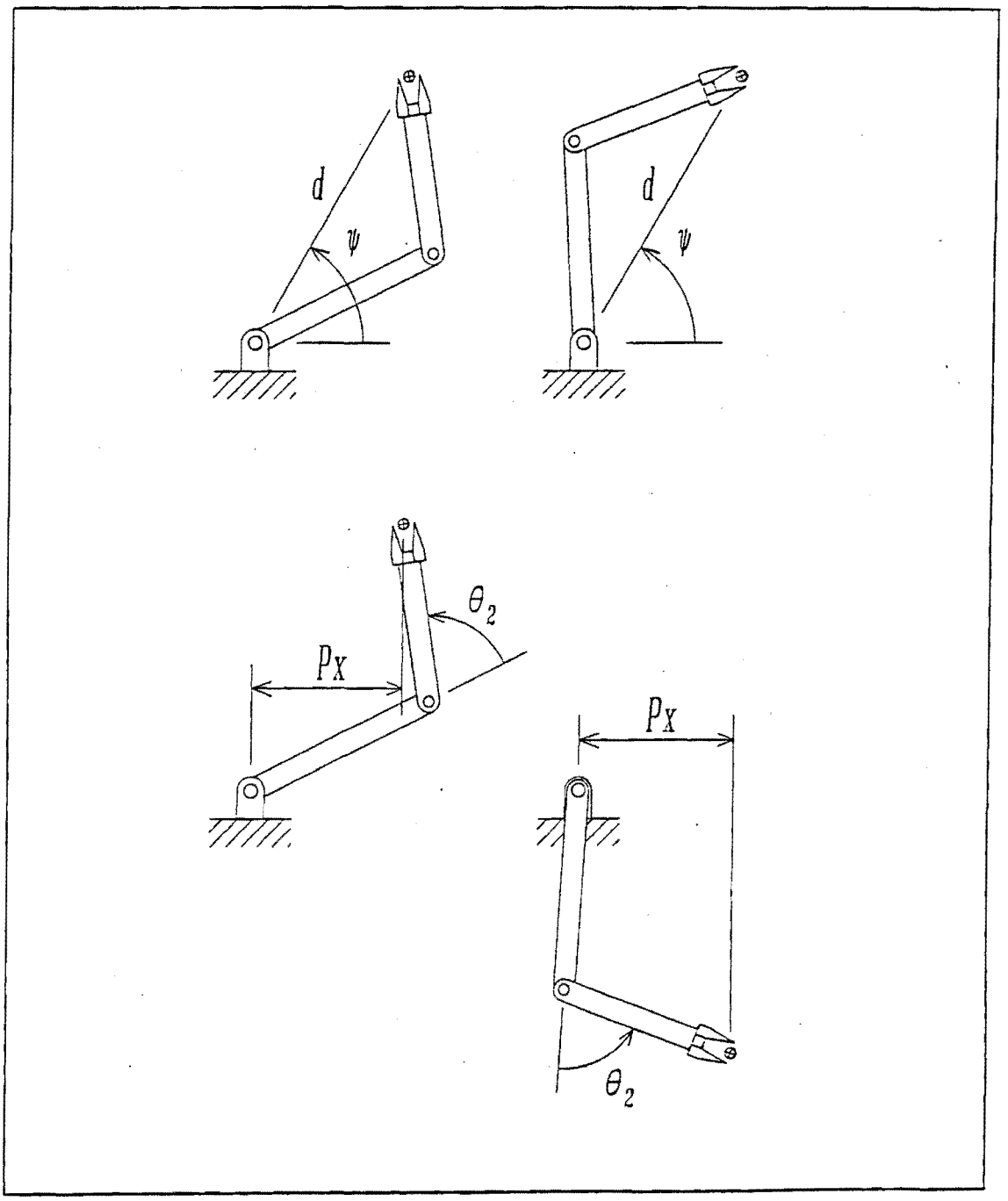

Figure 3.4: Solutions for Alternative Input Specification Sets

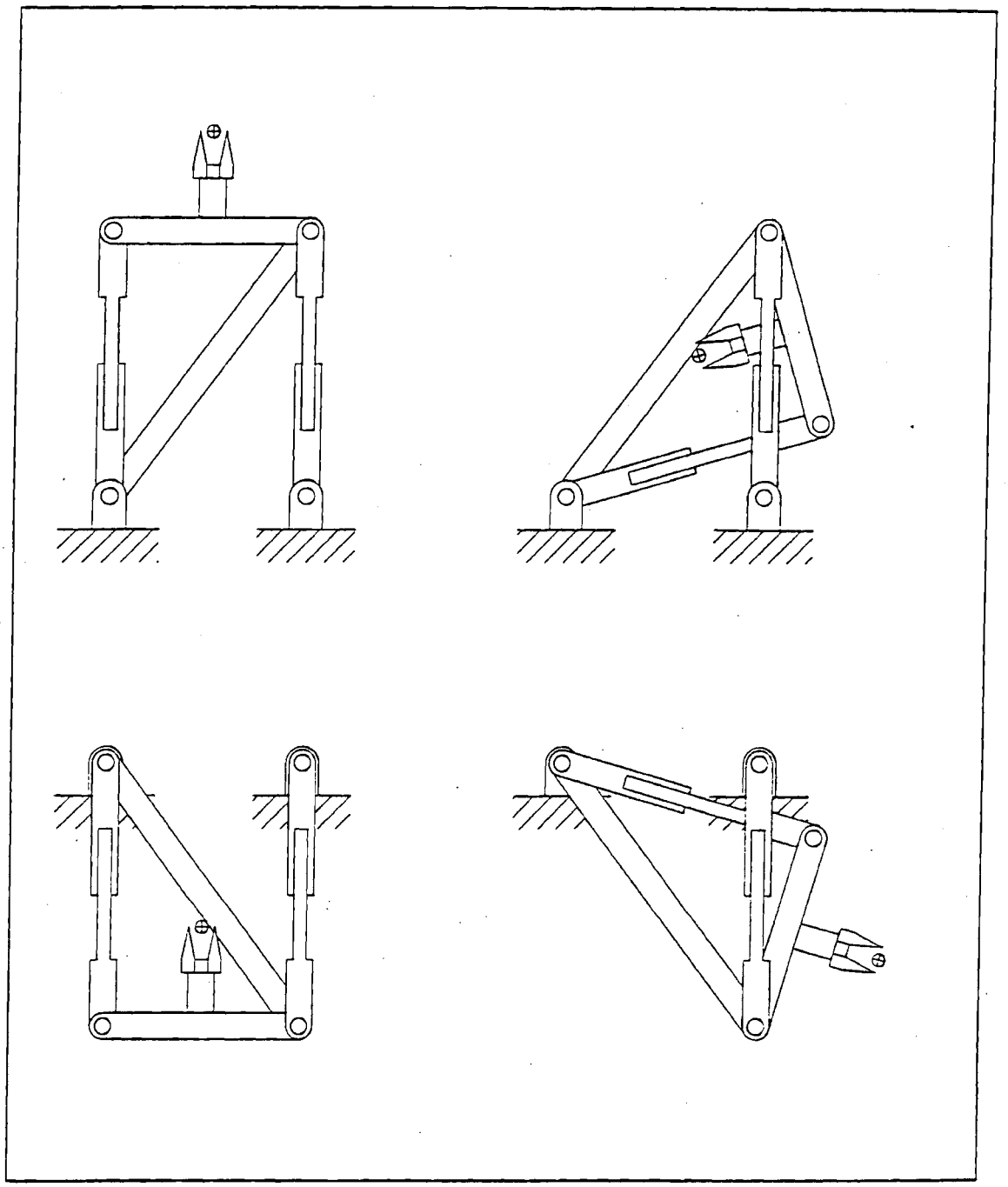

Figure 3.5: Four Solutions to the Conventional Forward Kinematic Analysis of a Simple Parallel Manipulator.

input specification set results in a non-linear forward solution. Consider the following canonical input parameter set. If it is assumed that the input to the system is ψ_1 and ψ_2, then a unique closed-form solution to the forward kinematics problem is obtained. If it is ever required to iteratively solve the forward kinematics in search of a particular result, it is logical to chose the parameter-specification set that results in linear solutions. Once the solution is found it is easy to calculate the corresponding unique values of l_1 and l_2.

Note that, if the conventional input specification set is used, the partial derivatives of the outputs with respect to the inputs ($\frac{\partial P_x}{\partial l_1}$, $\frac{\partial P_x}{\partial l_2}$, $\frac{\partial P_y}{\partial l_1}$, and $\frac{\partial P_y}{\partial l_2}$) cannot be expressed in closed form. The output parameters are not differentiable with respect to the inputs because of the non-linearities present in this forward problem. However, it is possible to use the alternate input specification set to find $\frac{\partial P_x}{\partial \psi_1}$, $\frac{\partial P_x}{\partial \psi_2}$, $\frac{\partial P_y}{\partial \psi_1}$, and $\frac{\partial P_y}{\partial \psi_2}$ in closed form. Similarly, $\frac{\partial \psi_1}{\partial l_1}$, $\frac{\partial \psi_2}{\partial l_2}$, $\frac{\partial \psi_1}{\partial l_1}$, and $\frac{\partial \psi_2}{\partial l_2}$ may also be expressed in closed form. It is now trivial to use the chain rule to compute the partial derivatives of goal positions with respect to changes in link lengths in closed form.

Although the method of utilizing a canonical input specification will not be necessary for all of the parallel geometries, it will be employed as part of the solution method for the inverse solution of the double-octahedral geometries.

3.3 Analysis of a Tetrahedral Module

The tetrahedral unit cell of Figure 3.1 represents the simplest possible spatial truss configuration. The basic unit cell consists of four non-coplanar nodes, each of which is joined to all other nodes by a side member. Thus, a tetrahedron has four triangular facets. Each facet shares one side member with all other facets. Imposing the restriction that all active modules must have two static triangular faces (this is necessary to provide an attachment surface) leaves only one remaining side member as a candidate for actuation. This essentially produces a single degree-of-freedom "hinge", or revolute actuator. The chosen geometry for the modular manipulator is illustrated in Figure 3.6. It consists of five static-length members and one variable-length member joined together with spheric joints at the four non-coplanar nodes, n_1,n_2,n_3, and n_4. For this work, it is assumed that all of the static length members except $n_2 - n_3$ are of length L_1, $n_2 - n_3$ is of length L_2, and the length of the actuated member will be denoted by l. This configuration was chosen to produce isosceles fixed triangles to which static trusses, with the same end condition, may be attached. A more general case, with scalene triangles could be analyzed; however, this geometry tends to produce forces that shear the two static trusses in opposite directions. This occurs anytime the line between n_1 and n_4 is not perpendicular to the hinge line $n_2 - n_3$. This shearing action is detrimental to the specified objective of the manipulator system.

A configuration with equilateral triangles is addressed by the present analysis

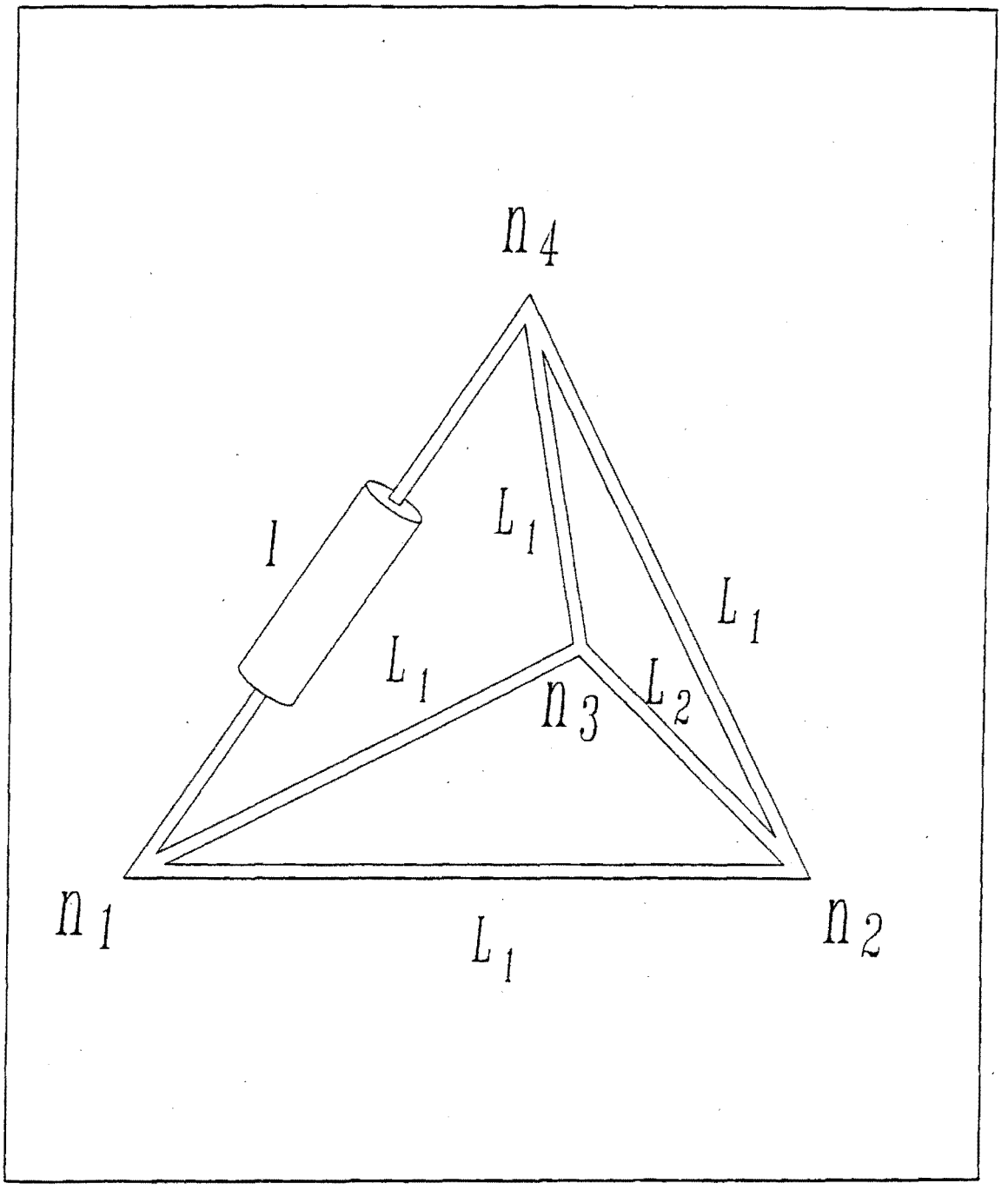

Figure 3.6: Active Tetrahedral Truss Module

if $L_1 = L_2$.

3.3.1 Forward and Inverse Kinematic Analysis

The forward kinematic problem for the tetrahedral truss can be stated as follows: *given the fixed lengths, L_1 and L_2, and the input length, l, find the angle θ that describes the relative rotation between the two fixed triangles.*

Likewise, the corresponding inverse kinematic problem may be summarized as: *given the desired rotation between the two fixed triangles, find the extensible link length l that produces this rotation.*

Figure 3.7 schematically illustrates an active tetrahedral truss module with the parameters needed to compute the forward and inverse kinematics. First, the height, or altitude, of the static triangles must be calculated as follows:

$$h = \sqrt{L_1^2 - \frac{L_2^2}{4}} \tag{3.1}$$

Now the angle θ can be found from the law of cosines as:

$$\theta = \arccos(1 - \frac{l^2}{2h^2}) = \arccos(1 - \frac{l^2}{2L_1^2 - \frac{1}{2}L_2^2}) \tag{3.2}$$

Rearranging this same equation yields a solution to the inverse kinematic problem.

$$l = \sqrt{2h^2(1 - \cos\theta)} = \sqrt{(2L_1^2 - \frac{1}{2}L_2^2)(1 - \cos\theta)} \tag{3.3}$$

Note that this single degree-of-freedom device has both a closed form forward and inverse solution. The forward solution is non-linear, and hence results in two possible solutions ($\pm\theta$). The inverse solution is linear and therefore results in a unique solution.

To efficiently utilize this result in solving a multi-module truss requires that the input/output relationship of all geometries be specified in the same manner. Although this last step appears to unnecessarily complicate the tetrahedral solution, it is fundamental to the development of a general multi-module kinematics algorithm. To establish this input/output relationship, a base coordinate frame, $\mathcal{B}$, will always be attached at the centroid of one fixed triangle. The X and Y axes of frame $\mathcal{B}$ are constrained to lie within the plane defined by $\Delta n_1 n_2 n_3$, with the X axis parallel to $n_2 n_3$. A second coordinate frame, $\mathcal{T}$, is attached in a similar manner to $\Delta n_1 n_2 n_4$. The positional relationship between these two frames is completely described by a homogeneous transform, ${}^{\mathcal{B}}_{\mathcal{T}}T$. For this particular geometry, this is only a function of θ, and may be written as:

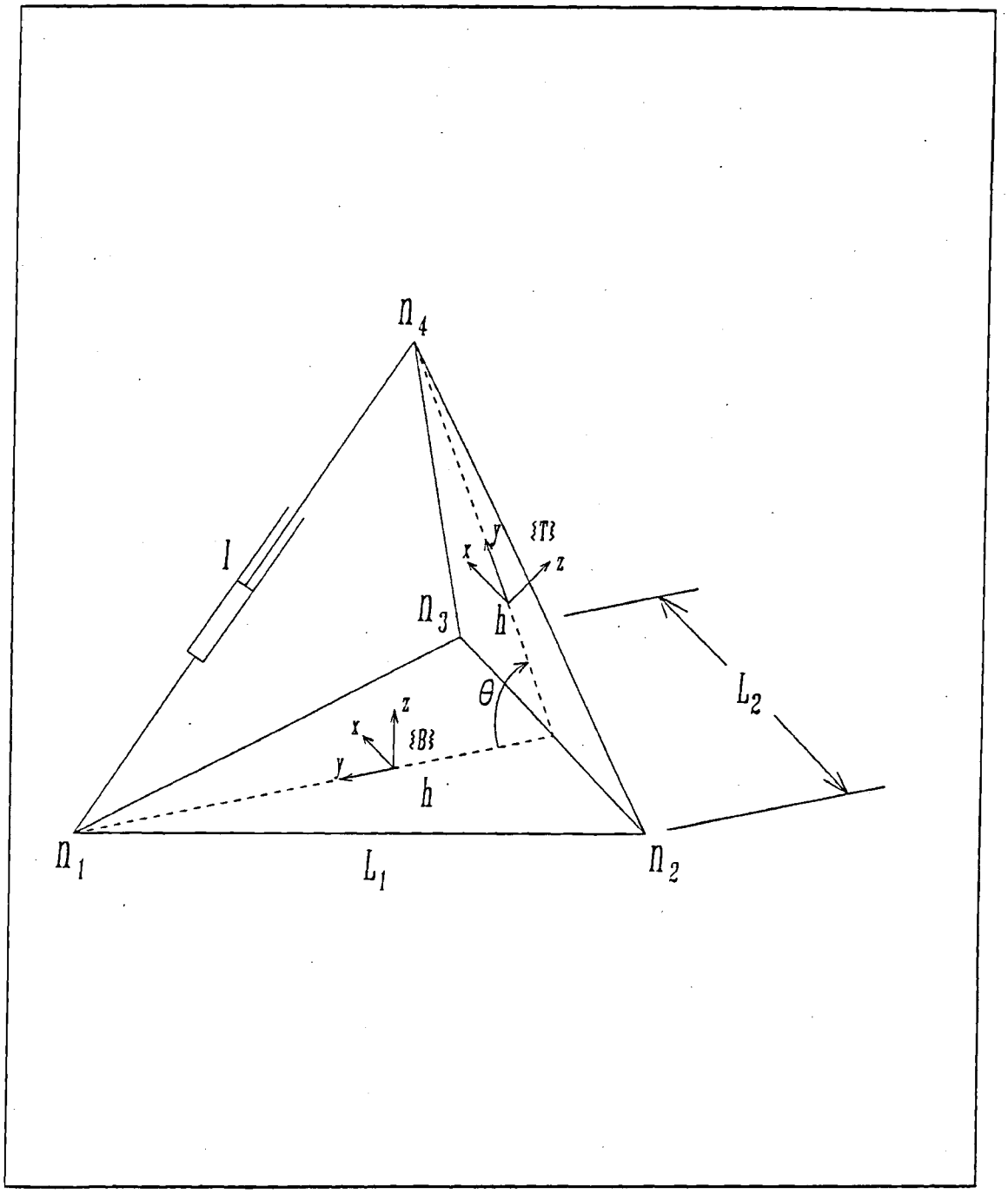

Figure 3.7: Schematic Tetrahedral Module with Analysis Parameters

$$ {}^{\mathcal{B}}_{\mathcal{T}}T(\theta) = \begin{bmatrix} 1 & 0 & 0 & 0 \\ 0 & \cos\theta & -\sin\theta & -\frac{h}{3}(1-\cos\theta) \\ 0 & \sin\theta & \cos\theta & \frac{h}{3}\sin\theta \\ 0 & 0 & 0 & 1 \end{bmatrix} \tag{3.4} $$

3.4 Analysis of a Longeron-Actuated, Octahedral Module

The most general form of a longeron-actuated, octahedral-based VGT module is illustrated in Figure 3.8. This specific geometry is often referred to as a Stewart platform manipulator. This active truss consists of six static-length members and six variable-length members which are joined together at six nodes $(n_1, n_2, \ldots, n_6)$ with spheric joints. The fixed-length members are joined together in sets of three to form two triangles. For convenience, it can be assumed without loss of generality that the static-length members are of equal lengths, and thus form two equilateral triangles. These two equilateral triangles will form the interface between the static and active truss modules. Other geometries for these two triangles are possible. These cases can be analyzed using the same procedures outlined below, with only slight notational modifications. One of the static triangles is used to define the base plane and has coordinate frame $\mathcal{B}$ at its centroid. The other triangle will form the top plane, with frame $\mathcal{T}$ at its centroid. The length of the extensible members will be denoted by the control variables $l_1, l_2, \ldots, l_6$. In this analysis, all fixed length members are assumed to be of length L. By assigning different values to the six control variables, the position and orientation of frame $\mathcal{T}$ relative to frame $\mathcal{B}$ can be altered. This relative position and orientation is described with six parameters. Three will be reserved for the x, y, and z position of frame $\mathcal{T}$ in frame $\mathcal{B}$ as described by the vector ${}^{\mathcal{B}}\vec{P}_{\mathcal{T}}$. The three remaining parameters will describe the orientation of $\mathcal{T}$ relative to $\mathcal{B}$. This is done by utilizing the standard roll-pitch-yaw notation; where roll is a rotation about the X-axis of frame $\mathcal{B}$ by γ, pitch is a rotation about the Y-axis of frame $\mathcal{B}$ by β, and yaw is a rotation about the Z-axis of frame $\mathcal{B}$ by α. This rotation of frame $\mathcal{T}$ relative to $\mathcal{B}$ can be compactly expressed as ${}^{\mathcal{B}}_{\mathcal{T}}R_{\gamma\beta\alpha}$, a 3×3 matrix possessing three independent variables.

It should be noted that it is also possible to construct a longeron-actuated, octahedral module with fewer than six extensible links. This is the case where one or more actuated longeron members are substituted with static-length members. For this degenerate Stewart platform case, the forward kinematics proceed as usual. However, the inverse problem is somewhat complicated, since the specified goal position and orientation must first be constrained to lie within the subspace of the manipulator.

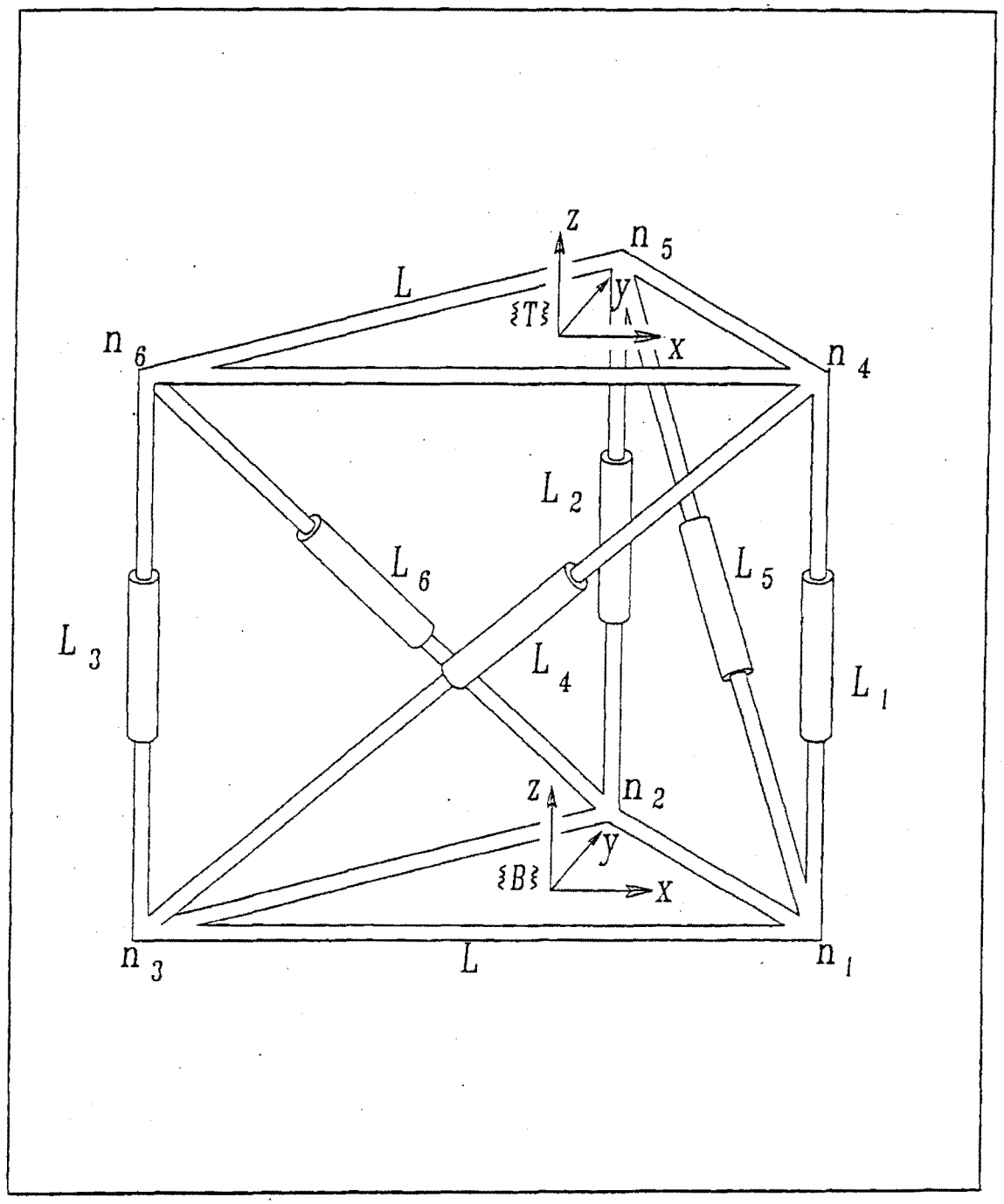

Figure 3.8: General, Longeron-Actuated, VGT Module (A Stewart Platform)

The following sections will present solutions to the forward and inverse kinematics of this manipulator.

3.4.1 Forward Kinematic Analysis

The forward kinematic analysis problem for the longeron-actuated, octahedral truss can be posed as follows:

Given the lengths of the longeron members (static or extensible), $l_1, l_2, \ldots, l_6$, solve for the position and orientation of frame $\mathcal{T}$ relative to frame $\mathcal{B}$.

In general, for this configuration of manipulator, this problem cannot be solved in closed form [17]. Instead, an iterative procedure has been developed that converges to a solution in a small number of iterations. This solution is generally more accurate than can be physically measured or controlled.

To assist in the forward kinematic analysis, it is helpful to employ the concept of kinematically equivalent devices. Two devices are said to be kinematically equivalent with respect to a point if both devices exhibit exactly the same motion characteristics for that point. Note that the two devices need not be structurally equivalent. This concept will simplify the mathematics involved and will aid in the visualization of the forward kinematic analysis.

Figurere 3.9 depicts the kinematically equivalent device that will be substituted for the side triangle $\triangle n_3 n_1 n_4$. In this case, two spheric joints and two prismatic joints (Figure 3.9-A) have been replaced by one cylindric joint and one prismatic joint (Figure 3.9-B). The cylindric joint is positioned along its axis, $\hat{u}_1$, at the point b_1. An explicit expression for $\vec{b}_1$ can be found as follows:

$$\psi_1 = \arccos\left(\frac{L^2 + l_4^2 - l_1^2}{2Ll_4}\right), \tag{3.5}$$

therefore,

$$\vec{b}_1 = \vec{n}_3 + l_4 \cos\psi_1 \hat{u}_1. \tag{3.6}$$

Now h_1, the altitude of triangle $\triangle n_3 n_1 n_4$,can be found.

$$h_1 = l_4 \sin\psi_1. \tag{3.7}$$

This is equivalent to the extension of the prismatic member that is shown in Figure 3.9-B. The unit vector $\hat{v}_1$ is defined to be normal to $\hat{u}_1$ and is constrained to lie in the plane of $\triangle n_1 n_2 n_3$. Now the point n_4 can be located as follows:

$$\vec{n}_4 = \vec{b}_1 + h_1 R_{[\hat{u}_1, \phi_1]} \hat{v}_1; \tag{3.8}$$

where $R_{[\hat{u}_1, \phi_1]}\hat{v}_1$ represents a rotation of $\hat{v}_1$ about $\hat{u}_1$ by an amount ϕ_1. Examination of the four previous equations reveals that $\vec{n}_4$ is a function dependent only on L, L_1, l_4, and ϕ_1. For the forward kinematics problem, $L, l_1, l_2, \ldots, l_6$ are known.

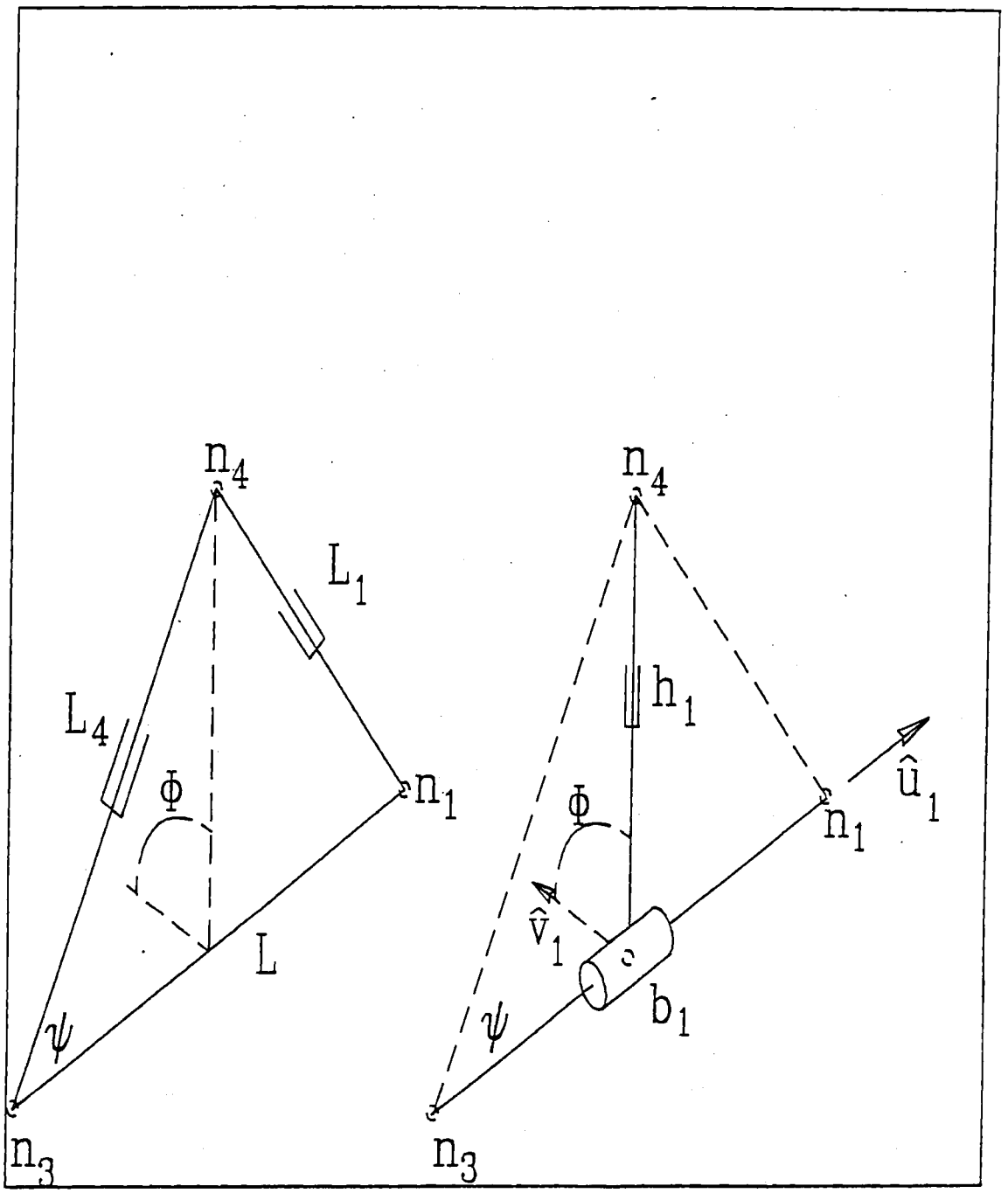

Figure 3.9: Kinematically Equivalent Devices Used for Analysis

Therefore, the vector $\vec{n}_4$ is only dependent on the unknown ϕ_1. Similar results can be obtained for the other two side triangles. These results are now summarized below:

$$\begin{aligned}
\vec{n}_4 &= \vec{n}_3 + l_4 \cos\psi_1 \hat{u}_1 + l_4 \sin\psi_1 R_{[\hat{u}_1,\phi_1]}\hat{v}_1, \\
\vec{n}_5 &= \vec{n}_1 + l_5 \cos\psi_2 \hat{u}_2 + l_5 \sin\psi_2 R_{[\hat{u}_2,\phi_2]}\hat{v}_2, \\
\vec{n}_6 &= \vec{n}_2 + l_6 \cos\psi_3 \hat{u}_3 + l_6 \sin\psi_3 R_{[\hat{u}_3,\phi_3]}\hat{v}_3;
\end{aligned} \tag{3.9}$$

where

$$\psi_2 = \arccos\left(\frac{L^2 + l_5^2 - l_2^2}{2Ll_5}\right), \tag{3.10}$$

$$\psi_3 = \arccos\left(\frac{L^2 + l_6^2 - l_3^2}{2Ll_6}\right). \tag{3.11}$$

The distance between nodes of the top triangle can now be found for any assumed set of ϕ's as:

$$\begin{aligned}
D_1 &= \|\vec{n}_4 - \vec{n}_5\| = \sqrt{(\vec{n}_4 - \vec{n}_5)\cdot(\vec{n}_4 - \vec{n}_5)}, \\
D_2 &= \|\vec{n}_5 - \vec{n}_6\| = \sqrt{(\vec{n}_5 - \vec{n}_6)\cdot(\vec{n}_5 - \vec{n}_6)}, \\
D_3 &= \|\vec{n}_6 - \vec{n}_4\| = \sqrt{(\vec{n}_6 - \vec{n}_4)\cdot(\vec{n}_6 - \vec{n}_4)}.
\end{aligned} \tag{3.12}$$

It is now necessary to check for closure. In order to have a valid assembly, the nodes of the top triangle must be a distance L apart. Thus, the following three equations must be satisfied:

$$\begin{aligned}
f_1(\phi_1, \phi_2) &= D_1 - L = 0, \\
f_2(\phi_2, \phi_3) &= D_2 - L = 0, \\
f_3(\phi_3, \phi_1) &= D_3 - L = 0.
\end{aligned} \tag{3.13}$$

This can be done simply by applying a Newton-Raphson root-finding algorithm that centers around the following linearization:

$$\begin{bmatrix} \frac{\partial f_1}{\partial \phi_1} & \frac{\partial f_1}{\partial \phi_2} & 0 \\ 0 & \frac{\partial f_2}{\partial \phi_2} & \frac{\partial f_2}{\partial \phi_3} \\ \frac{\partial f_3}{\partial \phi_1} & 0 & \frac{\partial f_3}{\partial \phi_3} \end{bmatrix} \begin{bmatrix} \Delta\phi_1 \\ \Delta\phi_2 \\ \Delta\phi_3 \end{bmatrix} = \begin{bmatrix} -f_1 \\ -f_2 \\ -f_3 \end{bmatrix}. \tag{3.14}$$

For any given iteration, $\Delta\phi_1, \Delta\phi_2$, and $\Delta\phi_3$ can be found, and the current "guessed" position can be modified by:

$$\begin{aligned} \phi_{1_{new}} &= \phi_{1_{old}} + \sigma(\Delta\phi_1), \\ \phi_{2_{new}} &= \phi_{2_{old}} + \sigma(\Delta\phi_2), \\ \phi_{3_{new}} &= \phi_{3_{old}} + \sigma(\Delta\phi_3). \end{aligned}$$

where σ is a damping factor added to avoid overshoot and speed convergence. In typical operation, with $\sigma = 0.90$, this procedure converges within an acceptable range after only four iterations. Other more efficient non-linear equation-solving routines could also be implemented. Upon convergence of the routine outlined above, the positions of nodes n_4, n_5, and n_6 are known. The origin of frame $\mathcal{T}$ can now be described in frame $\mathcal{B}$ as the centroid of these three nodes.

$$^{\mathcal{B}}\vec{P}_{\mathcal{T}} = \frac{(\vec{n}_4 + \vec{n}_5 + \vec{n}_6)}{3}. \tag{3.15}$$

The three unit vectors which form the coordinate axes of frame $\mathcal{T}$ can be described in frame $\mathcal{B}$ as follows:

$$^{\mathcal{B}}\hat{X}_{\mathcal{T}} = \frac{(\vec{n}_4 - \vec{n}_6)}{||\vec{n}_4 - \vec{n}_6||}, \tag{3.16}$$

$$^{\mathcal{B}}\hat{Z}_{\mathcal{T}} = \frac{(\vec{n}_4 - \vec{n}_6) \times (\vec{n}_5 - \vec{n}_6)}{||\,(\vec{n}_4 - \vec{n}_6) \times (\vec{n}_5 - \vec{n}_6)\,||}, \tag{3.17}$$

$$^{\mathcal{B}}\hat{Y}_{\mathcal{T}} = {}^{\mathcal{B}}\hat{Z}_{\mathcal{T}} \times {}^{\mathcal{B}}\hat{X}_{\mathcal{T}}. \tag{3.18}$$

Note that each of the above expressions is a vector quantity and, as such, each has three components. Now a rotation matrix describing the orientation of frame $\mathcal{T}$ with respect to frame $\mathcal{B}$ is given by:

$$^{\mathcal{B}}_{\mathcal{T}}R_{\gamma,\beta,\alpha} = \begin{bmatrix} ^{\mathcal{B}}\hat{X}_{\mathcal{T}x} & ^{\mathcal{B}}\hat{Y}_{\mathcal{T}x} & ^{\mathcal{B}}\hat{Z}_{\mathcal{T}x} \\ ^{\mathcal{B}}\hat{X}_{\mathcal{T}y} & ^{\mathcal{B}}\hat{Y}_{\mathcal{T}y} & ^{\mathcal{B}}\hat{Z}_{\mathcal{T}y} \\ ^{\mathcal{B}}\hat{X}_{\mathcal{T}z} & ^{\mathcal{B}}\hat{Y}_{\mathcal{T}z} & ^{\mathcal{B}}\hat{Z}_{\mathcal{T}z} \end{bmatrix}; \tag{3.19}$$

where each column of the matrix contains the x, y, and z components of each coordinate axis that composes frame $\mathcal{T}$. If desired, this expression can now be equated to the standard roll-pitch-yaw representation of the rotation matrix as presented below:

$$ {}^{\mathcal{B}}_{\mathcal{T}}R_{\gamma,\beta,\alpha} = \begin{bmatrix} c\alpha c\beta & c\alpha s\beta s\gamma - s\alpha c\gamma & c\alpha s\beta c\gamma + s\alpha s\gamma \\ s\alpha c\beta & s\alpha s\beta s\gamma + c\alpha c\gamma & s\alpha s\beta c\gamma - c\alpha s\gamma \\ -s\beta & c\beta s\gamma & c\beta c\gamma \end{bmatrix}; \tag{3.20} $$

where $c\beta = \cos\beta, s\beta = \sin\beta$, etc.

The roll-pitch-yaw description can now be obtained uniquely from one of the three following sets of relations [12, pages 41–42].

•Case 1. if $\left\| {}^{\mathcal{B}}\hat{X}_{\mathcal{T}z} \right\| \neq 1$,

$$ \begin{aligned} \gamma &= \mathrm{ATAN2}\left({}^{\mathcal{B}}\hat{Y}_{\mathcal{T}z}, {}^{\mathcal{B}}\hat{Z}_{\mathcal{T}z}\right) \\ \beta &= \mathrm{ATAN2}\left(-{}^{\mathcal{B}}\hat{X}_{\mathcal{T}z}, \sqrt{{}^{\mathcal{B}}\hat{X}^2_{\mathcal{T}x} + {}^{\mathcal{B}}\hat{X}^2_{\mathcal{T}y}}\right) \\ \alpha &= \mathrm{ATAN2}\left({}^{\mathcal{B}}\hat{X}_{\mathcal{T}y}, {}^{\mathcal{B}}\hat{X}_{\mathcal{T}x}\right) \end{aligned} \tag{3.21} $$

•Case 2. if ${}^{\mathcal{B}}\hat{X}_{\mathcal{T}z} = +1$,

$$ \begin{aligned} \gamma &= \mathrm{ATAN2}\left({}^{\mathcal{B}}\hat{Y}_{\mathcal{T}x}, {}^{\mathcal{B}}\hat{Y}_{\mathcal{T}y}\right) \\ \beta &= 90^o \\ \alpha &= 0 \end{aligned} \tag{3.22} $$

•Case 3. if ${}^{\mathcal{B}}\hat{X}_{\mathcal{T}z} = -1$,

$$ \begin{aligned} \gamma &= -\mathrm{ATAN2}\left({}^{\mathcal{B}}\hat{Y}_{\mathcal{T}x}, {}^{\mathcal{B}}\hat{Y}_{\mathcal{T}y}\right) \\ \beta &= -90^o \\ \alpha &= 0 \end{aligned} \tag{3.23} $$

The results of the forward kinematic solution just presented are non-linear and hence no unique solution exists. In fact, for this particular truss, sixteen distinct assemblies, or branches, exist [2, 3]. These solutions represent mathematically acceptable solutions, some of which the truss could physically obtain, but only after unpinning the joints and reassembling the truss within a new branch. From

an operational standpoint, none of these solutions is practical. To result in a practical solution, this mathematical solution technique must somehow be tailored to omit all but the desired solution. This is most efficiently done by limiting the range of ϕ_1, ϕ_2, and ϕ_3 in the iterative procedure.

Historically, manipulators in which the kinematics must be solved iteratively have been avoided. This can primarily be attributed to convergence problems and, to a lesser degree, the speed at which these algorithms could be executed. It is true that for large moves, convergence of the proposed algorithms might present a problem. However, at the speed at which modern controllers can update a position, there is no need to move the system a great distance in one step. For small moves the values of ϕ_1, ϕ_2, and ϕ_3 are known relatively accurately to start with. Thus, convergence is not a problem unless singularities are present. Singularity points can be identified by forming a Jacobian matrix and setting its determinate equal to zero. However, this particular configuration can easily be designed such that the singularity points occur outside of the physical workspace, which is limited by the range of the extensible longerons.

3.4.2 Inverse Kinematic Analysis

The inverse kinematic analysis of the longeron-actuated, octahedral truss is both closed-form and linear. The inverse kinematic analysis problem can be stated as follows:

Given the position vector, $\vec{P}_1$, and α, β, γ, solve for the set of longeron lengths $\{l_1, l_2, \ldots, l_6\}$.

Since α, β, and γ are known, the rotation from $\mathcal{B}$ to $\mathcal{T}$ can be described by the rotation matrix

$$ {}^{\mathcal{B}}_{\mathcal{T}}R_{\gamma,\beta,\alpha} = \begin{bmatrix} c\alpha c\beta & c\alpha s\beta s\gamma - s\alpha c\gamma & c\alpha s\beta c\gamma + s\alpha s\gamma \\ s\alpha c\beta & s\alpha s\beta s\gamma + c\alpha c\gamma & s\alpha s\beta c\gamma - c\alpha s\gamma \\ -s\beta & c\beta s\gamma & c\beta c\gamma \end{bmatrix}. \tag{3.24} $$

A transform can now be defined that encompasses both the rotation and translation of $\mathcal{T}$ relative to $\mathcal{B}$. This transform is defined as:

$$ {}^{\mathcal{B}}_{\mathcal{T}}T = \begin{bmatrix} & [{}^{\mathcal{B}}_{\mathcal{T}}R] & & [{}^{\mathcal{B}}\vec{P}_1] \\ 0 & 0 & 0 & 1 \end{bmatrix}. \tag{3.25} $$

Nodes n_4, n_5, and n_6, which are known in $\mathcal{T}$, can now be described in $\mathcal{B}$.

$$ \begin{aligned} {}^{\mathcal{B}}\vec{n}_4 &= {}^{\mathcal{B}}_{\mathcal{T}}T^{\mathcal{T}}\vec{n}_4, \\ {}^{\mathcal{B}}\vec{n}_5 &= {}^{\mathcal{B}}_{\mathcal{T}}T^{\mathcal{T}}\vec{n}_5, \\ {}^{\mathcal{B}}\vec{n}_6 &= {}^{\mathcal{B}}_{\mathcal{T}}T^{\mathcal{T}}\vec{n}_6. \end{aligned} \tag{3.26} $$

Finally, the length of the extensible members can be solved for directly as the euclidean distance between appropriate nodes.

$$
\begin{aligned}
l_1 &= \left\| {}^{\mathcal{B}}\vec{n}_4 - {}^{\mathcal{B}}\vec{n}_1 \right\| = \sqrt{({}^{\mathcal{B}}\vec{n}_4 - {}^{\mathcal{B}}\vec{n}_1)\cdot({}^{\mathcal{B}}\vec{n}_4 - {}^{\mathcal{B}}\vec{n}_1)}, \\
l_2 &= \left\| {}^{\mathcal{B}}\vec{n}_5 - {}^{\mathcal{B}}\vec{n}_2 \right\| = \sqrt{({}^{\mathcal{B}}\vec{n}_5 - {}^{\mathcal{B}}\vec{n}_2)\cdot({}^{\mathcal{B}}\vec{n}_5 - {}^{\mathcal{B}}\vec{n}_2)}, \\
l_3 &= \left\| {}^{\mathcal{B}}\vec{n}_6 - {}^{\mathcal{B}}\vec{n}_3 \right\| = \sqrt{({}^{\mathcal{B}}\vec{n}_6 - {}^{\mathcal{B}}\vec{n}_3)\cdot({}^{\mathcal{B}}\vec{n}_6 - {}^{\mathcal{B}}\vec{n}_3)}, \\
l_4 &= \left\| {}^{\mathcal{B}}\vec{n}_4 - {}^{\mathcal{B}}\vec{n}_3 \right\| = \sqrt{({}^{\mathcal{B}}\vec{n}_4 - {}^{\mathcal{B}}\vec{n}_3)\cdot({}^{\mathcal{B}}\vec{n}_4 - {}^{\mathcal{B}}\vec{n}_3)}, \\
l_5 &= \left\| {}^{\mathcal{B}}\vec{n}_5 - {}^{\mathcal{B}}\vec{n}_1 \right\| = \sqrt{({}^{\mathcal{B}}\vec{n}_5 - {}^{\mathcal{B}}\vec{n}_1)\cdot({}^{\mathcal{B}}\vec{n}_5 - {}^{\mathcal{B}}\vec{n}_1)}, \\
l_6 &= \left\| {}^{\mathcal{B}}\vec{n}_6 - {}^{\mathcal{B}}\vec{n}_2 \right\| = \sqrt{({}^{\mathcal{B}}\vec{n}_6 - {}^{\mathcal{B}}\vec{n}_2)\cdot({}^{\mathcal{B}}\vec{n}_6 - {}^{\mathcal{B}}\vec{n}_2)}.
\end{aligned}
\tag{3.27}
$$

Note that there can only be one solution for the euclidean distance between two points. This means that in the absence of any other constraints, a unique solution for any specified position and orientation always exists. In reality, of course, other constraints do exist. The primary constraint for this device is the range of its variable-length members. The inverse kinematic results must be checked to ensure that they are within the physical range of the extensible links. If not, the given goal position is outside of the manipulators workspace and cannot be reached. To address the case where a truss may contain k static-length longerons, the inverse solution can proceed as usual. However, the final results (link lengths) must be checked to ensure that inverse analysis produces corresponding values acceptably close to the true static lengths. If not, the given goal position does not lie within the $(6-k)$-dimensional subspace of the manipulator.

3.5 Analysis of a General, Batten-Actuated, Double-Octahedral Module

Section 3.4 introduced an analysis procedure for a VGT geometry based on an octahedral unit cell structure. This section will examine an active truss geometry, again based on the octahedral unit cell structure. This structure consists simply of two octahedra sharing a common triangular facet. For this reason it is referred to as a double-octahedral geometry. Although many possible choices exist for how to actuate this truss structure, this work will address only trusses in which the midplane battens are actuated. This general class of VGT manipulator has been shown to posses a good compromise between high strength and useful workspace.[4] [62, 63] Figure 3.10 illustrates a batten-actuated VGT module. Note that the

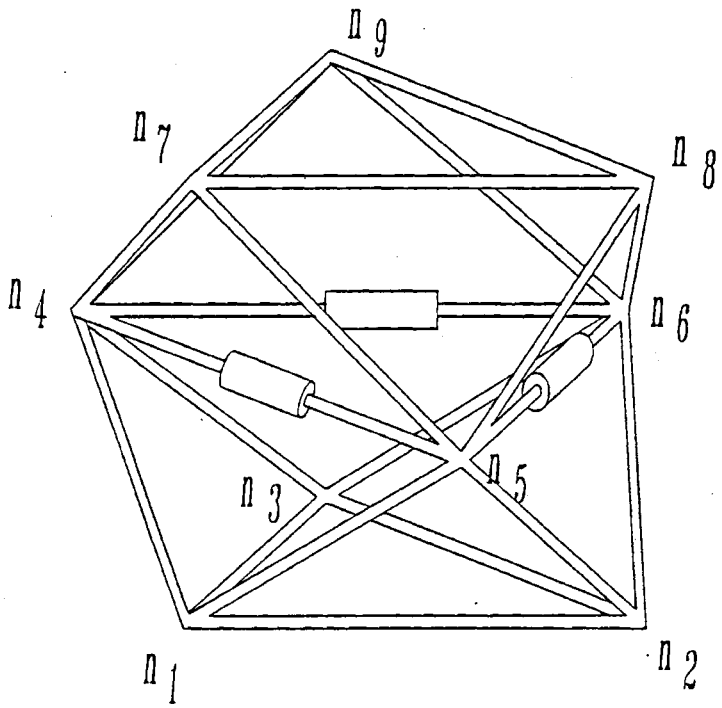

Link Identification

Link	Between Nodes
l_1	$n_4 - n_5$
l_2	$n_5 - n_6$
l_3	$n_6 - n_4$
L_1	$n_1 - n_4$
L_2	$n_2 - n_5$
L_3	$n_3 - n_6$
L_4	$n_3 - n_4$
L_5	$n_1 - n_5$
L_6	$n_2 - n_6$
L_7	$n_5 - n_7$
L_8	$n_6 - n_8$
L_9	$n_4 - n_9$
L_{10}	$n_4 - n_7$
L_{11}	$n_5 - n_8$
L_{12}	$n_6 - n_9$

Figure 3.10: Batten Actuated, Double-Octahedral VGT Module

top and bottom batten triangles are defined by fixed-length members. These two triangles will serve as the attachment points for the static truss sections. The nodes of the truss are numbered n_1, n_2, ..., n_9 as shown in Figure 3.10. The fixed length members of the base and top planes will be of length L_{Base} and L_{Top} respectively. The length of the extensible links will again be denoted by the lowercase variables l_1, l_2, and l_3. For this general analysis, it will be assumed that the fixed-length longeron members can be of different lengths. These lengths will be identified as $L_1, L_2, \ldots, L_{12}$.

Since this truss configuration is again based on an octahedral unit cell, the kinematic analysis is similar to the longeron-actuated octahedron previously presented. Because of this inherent similarity, the following forward and inverse kinematic discussions will be somewhat abbreviated. For further clarifications, refer back to Section 3.4.

3.5.1 Forward Kinematic Analysis

The forward kinematic problem for this active module may be summarized as follows: *given the lengths of the fixed length members ($L_1, \ldots, L_{12}$), and the lengths of the extensible members (l_1, l_2, and l_3), find the position and orientation of frame $\mathcal{T}$ relative to frame $\mathcal{B}$.*

Again, the concept of a kinematically equivalent device will greatly simplify the analysis of the octahedron. The kinematic equivalent to the first octahedral cell of the double-octahedral truss is shown in Figure 3.11-A.

By analogy to the previous octahedral analysis, the positions of the midplane nodes(n_4, n_5, n_6),can be identified as a function of the unknowns ϕ_1, ϕ_2, and ϕ_3.

$$\begin{aligned}
\vec{n}_4 &= \vec{n}_3 + L_4 \cos\psi_1 \hat{u}_1 + L_4 \sin\psi_1 R_{[\hat{u}_1,\phi_1]}\hat{v}_1, \\
\vec{n}_5 &= \vec{n}_1 + L_5 \cos\psi_2 \hat{u}_2 + L_5 \sin\psi_2 R_{[\hat{u}_2,\phi_2]}\hat{v}_2, \\
\vec{n}_6 &= \vec{n}_2 + L_6 \cos\psi_3 \hat{u}_3 + L_6 \sin\psi_3 R_{[\hat{u}_3,\phi_3]}\hat{v}_3;
\end{aligned} \tag{3.28}$$

where

$$\psi_1 = \arccos\left(\frac{L_{Base}^2 + L_4^2 - L_1^2}{2L_{Base}L_4}\right), \tag{3.29}$$

$$\psi_2 = \arccos\left(\frac{L_{Base}^2 + L_5^2 - L_2^2}{2L_{Base}L_5}\right), \tag{3.30}$$

$$\psi_3 = \arccos\left(\frac{L_{Base}^2 + L_6^2 - L_3^2}{2L_{Base}L_6}\right). \tag{3.31}$$

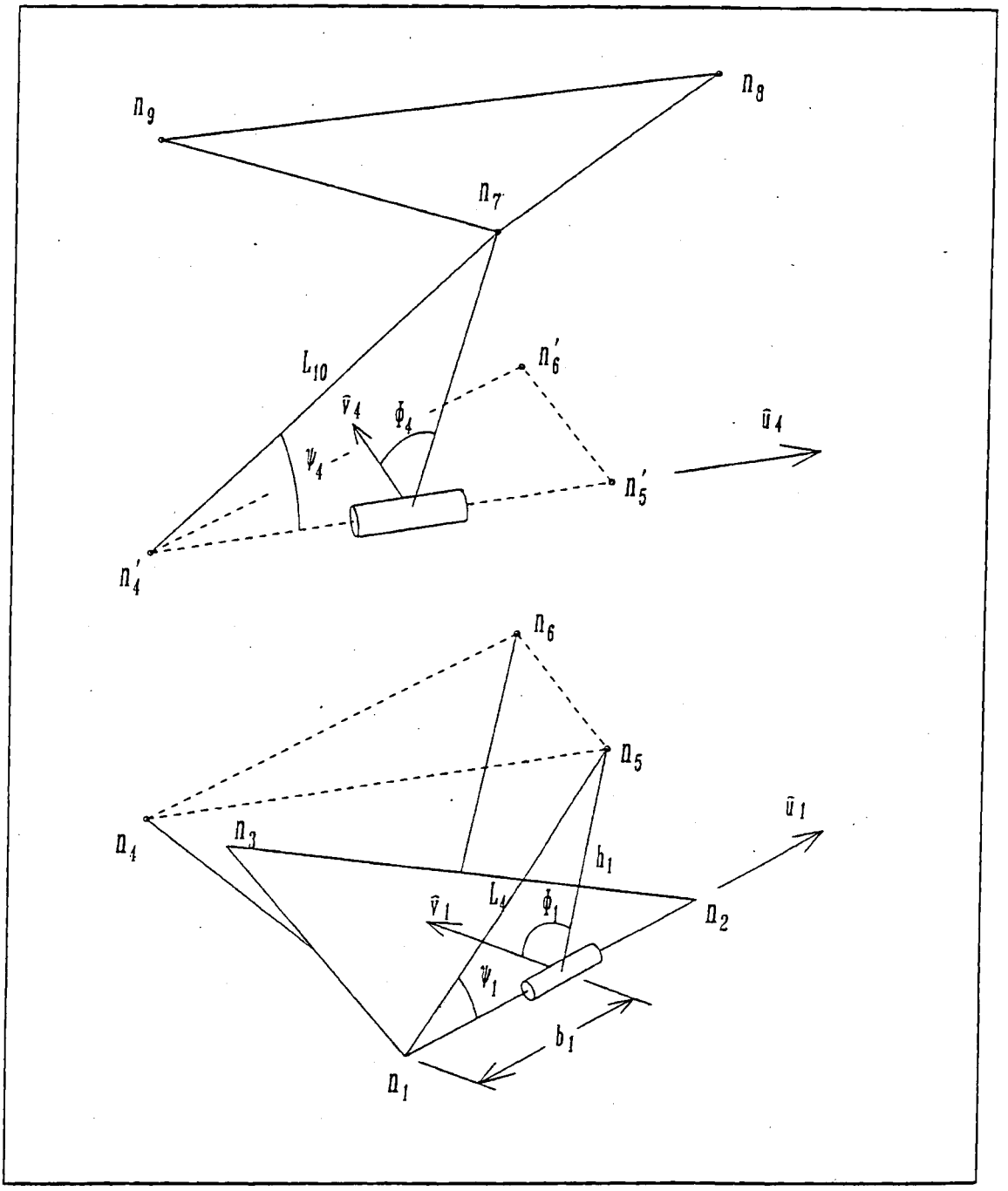

Figure 3.11: Kinematic Equivalent to the Batten-Actuated, Double-Octahedral VGT

The distance between nodes of the midplane triangle can now be found for any given ϕ_1, ϕ_2, and ϕ_3 as:

$$\begin{aligned} D_1 &= \|\vec{n}_4 - \vec{n}_5\| = \sqrt{(\vec{n}_4 - \vec{n}_5)\cdot(\vec{n}_4 - \vec{n}_5)}, \\ D_2 &= \|\vec{n}_5 - \vec{n}_6\| = \sqrt{(\vec{n}_5 - \vec{n}_6)\cdot(\vec{n}_5 - \vec{n}_6)}, \\ D_3 &= \|\vec{n}_6 - \vec{n}_4\| = \sqrt{(\vec{n}_6 - \vec{n}_4)\cdot(\vec{n}_6 - \vec{n}_4)}. \end{aligned} \tag{3.32}$$

It is now necessary to check for closure. In order to have a valid assembly, the nodes of the midplane triangle must be the specified distance apart. Thus, the following three equations must be satisfied:

$$\begin{aligned} f_1(\phi_1, \phi_2) &= D_1 - l_1 = 0, \\ f_2(\phi_2, \phi_3) &= D_2 - l_2 = 0, \\ f_3(\phi_3, \phi_1) &= D_3 - l_3 = 0. \end{aligned} \tag{3.33}$$

The Newton-Raphson root-finding algorithm may now be applied exactly as it was for the longeron-actuated truss. Upon convergence, a feasible set of ϕ_1, ϕ_2, and ϕ_3 is obtained. These must be checked to ensure that the solution is in the proper branch.

At this stage of the analysis, the positions of the three midplane nodes are known. As a practical consideration, all of the double-octahedral VGT cells constructed to date have contained a mid-plane joint offset. This deviation from ideal truss design is necessary to ensure an adequate range of motion for the truss joint. In addition, incorporating this offset into the design avoids the complications involved in having five co-located spheric joints. If a mid-plane joint offset is present, this distance can easily be included in the analysis by forming three additional midplane nodes (n'_4, n'_5, and n'_6) that are displaced the amount of the offset in a direction normal to the midplane. The solution for the second octahedron is obtained by essentially repeating the solution procedure above. One possible kinematic equivalent to the second octahedral cell is shown in Figure 3.11-B. Note that $\hat{u}_4$, $\hat{u}_5$, and $\hat{u}_6$ are defined by the position of the midplane nodes. These unit vectors may be described in the base coordinate frame, $\mathcal{B}$, as:

$$\hat{u}_4 = \frac{\vec{n}_5 - \vec{n}_4}{l_1} \tag{3.34}$$

$$\hat{u}_5 = \frac{\vec{n}_6 - \vec{n}_5}{l_2} \tag{3.35}$$

$$\hat{u}_6 = \frac{\vec{n}_4 - \vec{n}_6}{l_3} \tag{3.36}$$

The unit vectors $\hat{v}_4$, $\hat{v}_5$, and $\hat{v}_6$ must also be defined such that they lie within the midplane, perpendicular to the corresponding actuated member. This is most easily accomplished by defining another unit vector, $\hat{w}$, that is normal to the midplane. Using the vector cross product,

$$\hat{w} = \frac{\hat{u}_5 \times (-\hat{u}_4)}{||\hat{u}_5 \times (-\hat{u}_4)||} \tag{3.37}$$

Now

$$\hat{v}_4 = \hat{w} \times \hat{u}_4 \tag{3.38}$$

$$\hat{v}_5 = \hat{w} \times \hat{u}_5 \tag{3.39}$$

$$\hat{v}_6 = \hat{w} \times \hat{u}_6 \tag{3.40}$$

The position of the top plane nodes may now be identified solely as a function of the unknowns ϕ_4, ϕ_5, and ϕ_6.

$$\begin{aligned} \vec{n}_7 &= \vec{n}'_4 + L_{10}\cos\psi_4\hat{u}_4 + L_{10}\sin\psi_4 R_{[\hat{u}_4,\phi_4]}\hat{v}_4, \\ \vec{n}_8 &= \vec{n}'_5 + L_{11}\cos\psi_5\hat{u}_5 + L_{11}\sin\psi_5 R_{[\hat{u}_5,\phi_5]}\hat{v}_5, \\ \vec{n}_9 &= \vec{n}'_6 + L_{12}\cos\psi_6\hat{u}_6 + L_{12}\sin\psi_6 R_{[\hat{u}_6,\phi_6]}\hat{v}_6; \end{aligned} \tag{3.41}$$

where

$$\psi_4 = \arccos\left(\frac{l_1^2 + L_{10}^2 - L_7^2}{2l_1L_{10}}\right), \tag{3.42}$$

$$\psi_5 = \arccos\left(\frac{l_2^2 + L_{11}^2 - L_8^2}{2l_2L_{11}}\right), \tag{3.43}$$

$$\psi_6 = \arccos\left(\frac{l_3^2 + L_{12}^2 - L_9^2}{2l_3L_{12}}\right). \tag{3.44}$$

The distance between nodes of the top plane triangle can now be found for any given ϕ_4, ϕ_5, and ϕ_6 as:

$$
\begin{aligned}
D_4 &= \|\vec{n}_7 - \vec{n}_8\| = \sqrt{(\vec{n}_7 - \vec{n}_8)\cdot(\vec{n}_7 - \vec{n}_8)}, \\
D_5 &= \|\vec{n}_8 - \vec{n}_9\| = \sqrt{(\vec{n}_8 - \vec{n}_9)\cdot(\vec{n}_8 - \vec{n}_9)}, \\
D_6 &= \|\vec{n}_9 - \vec{n}_7\| = \sqrt{(\vec{n}_9 - \vec{n}_7)\cdot(\vec{n}_{12} - \vec{n}_7)}.
\end{aligned} \tag{3.45}
$$

Again, it is necessary to check for closure. In order to have a valid assembly, the nodes of the top plane triangle must be the specified distance apart. Thus, the following three equations must be satisfied:

$$
\begin{aligned}
f_1(\phi_1, \phi_2) &= D_1 - L_{Top} = 0, \\
f_2(\phi_2, \phi_3) &= D_2 - L_{Top} = 0, \\
f_3(\phi_3, \phi_1) &= D_3 - L_{Top} = 0.
\end{aligned} \tag{3.46}
$$

The Newton-Raphson root-finding algorithm may again be applied. Upon convergence, a feasible set of ϕ_4, ϕ_5, and ϕ_6 is obtained. These must be checked to ensure the solution is in the proper branch.

The origin of frame $\mathcal{T}$ can now be described in frame $\mathcal{B}$ as the centroid of the top plane triangle.

$$
{}^{\mathcal{B}}\vec{P}_{\mathcal{T}} = \frac{(\vec{n}_7 + \vec{n}_8 + \vec{n}_9)}{3}. \tag{3.47}
$$

The three unit vectors that form the coordinate axes of frame $\mathcal{T}$ can be described in frame $\mathcal{B}$ as follows:

$$
{}^{\mathcal{B}}\hat{X}_{\mathcal{T}} = \frac{(\vec{n}_7 - \vec{n}_9)}{||\vec{n}_7 - \vec{n}_9||}, \tag{3.48}
$$

$$
{}^{\mathcal{B}}\hat{Z}_{\mathcal{T}} = \frac{(\vec{n}_7 - \vec{n}_9) \times (\vec{n}_8 - \vec{n}_9)}{||\,(\vec{n}_7 - \vec{n}_9) \times (\vec{n}_8 - \vec{n}_9)\,||}, \tag{3.49}
$$

$$
{}^{\mathcal{B}}\hat{Y}_{\mathcal{T}} = {}^{\mathcal{B}}\hat{Z}_{\mathcal{T}} \times {}^{\mathcal{B}}\hat{X}_{\mathcal{T}}. \tag{3.50}
$$

Now, the transformation matrix that describes frame $\mathcal{T}$ with respect to frame $\mathcal{B}$ is given by:

$$
{}^{\mathcal{B}}_{\mathcal{T}}T_{(l_1,l_2,l_3)} = \begin{bmatrix} {}^{\mathcal{B}}\hat{X}_{\mathcal{T}} & {}^{\mathcal{B}}\hat{Y}_{\mathcal{T}} & {}^{\mathcal{B}}\hat{Z}_{\mathcal{T}} & {}^{\mathcal{B}}\vec{P}_{\mathcal{T}} \\ 0 & 0 & 0 & 1 \end{bmatrix}. \tag{3.51}
$$

3.5.2 Inverse Kinematic Analysis

The inverse kinematic problem for the general batten-actuated VGT module may be stated as follows: *given the desired end condition of the active module, find the extensible link lengths, l_1, l_2, and l_3.*

This poses a slightly different problem from the other geometries discussed thus far. Note that, if a general six DOF position and orientation is specified, a solution is only possible if the goal lies within the three DOF subspace of the manipulator. Another possibility is to specify only three parameters. For example, the X, Y, and Z position of frame $\mathcal{T}$ relative to $\mathcal{B}$, ${}^{\mathcal{B}}\vec{P}_{\mathcal{T}}$, could be specified. Or the angular displacement about the $\hat{X}_{\mathcal{B}}$ and $\hat{Y}_{\mathcal{B}}$ axes may be specified in conjunction with a third positional parameter; either the X, Y, or Z position of $\mathcal{T}$ relative to $\mathcal{B}$. As a subtlety of this particular geometric configuration, a single truss module cannot effect any angular displacements about the $\hat{Z}_{\mathcal{B}}$ axis. For this reason, an advantageous way of specifying a goal orientation is to specify only a unit vector normal to the top plane, ${}^{\mathcal{B}}\hat{Q}$.

To solve the inverse kinematic problem for any of the above goal specifications, the forward solution must be iteratively solved until convergence is achieved. It would appear that a logical method for accomplishing this is to follow the algorithmic steps enumerated below.

1. Assume a set of l's.
2. Use the forward kinematics solution to calculate the resulting end condition.
3. Compare this to the desired end position. If converged, proceed to step 7.
4. Evaluate the effect of each l on each end parameter (e.g. $\frac{\partial x}{\partial l_1}$). This again requires solving the forward kinematics problem three times.
5. Compute a set of Δl's.
6. Modify the assumed set of l's and return to step 2.
7. Verify solution feasibility.

This procedure will indeed converge to an acceptable solution. However, the forward kinematics problem must be solved a total of four times for one iteration. The real problem here is that the forward kinematics problem is itself iterative. In the case of the general double-octahedral truss, solving both the first and second octahedra requires iterative loops. Thus, the above outlined procedure requires that eight iterative loops be processed with each pass.

Although this method does perform well in many situations, it can be dramatically improved by imposing some constraints on the design of the truss module. If, for example, the static-length links are all made the same length, a faster inverse kinematic analysis method can be employed. This design constraint may prove to be too restrictive for many applications. As a more general alternative, the restriction that will be exploited for this work is that of symmetry. Namely, that the fixed length members of the second octahedral cell must be the same length as their reflected members in the first octahedral cell. In this case, the plane of symmetry is the midplane.

3.5.3 Forward Kinematic Solutions with Symmetry Imposed

The midplane of the symmetric double-octahedral truss described above may be identified as outlined previously for the general double-octahedral. This requires an iterative procedure to find the mid-plane nodes. After the midplane is identified, the three base nodes may be projected through the midplane to form the three nodes of the top plane. See Figure 3.12. This projection process is closed-form and will be briefly discussed below.

In general, a projection, or mirroring, process can be carried out in closed form if the plane of symmetry is defined and the coordinates of the point to be mirrored are known. For this particular case, the plane of symmetry is defined by nodes n_4, n_5, and n_6, or, if appropriate, the midpoints of $n_4 - n_4'$, $n_5 - n_5'$, and $n_6 - n_6'$. Thus, a unit vector normal to this plane can be defined using the vector cross product.

$$\hat{U}_{\text{norm}} = \frac{(\vec{n}_5 - \vec{n}_4) \times (\vec{n}_6 - \vec{n}_4)}{||(\vec{n}_5 - \vec{n}_4) \times (\vec{n}_6 - \vec{n}_4)||} \tag{3.52}$$

Since the base nodes must be projected perpendicular to the plane of symmetry, their mirror images must lie along a vector which passes through the base node in question and points in the direction of $\hat{U}_{\text{norm}}$. Additionally, the mirrored node must lie the same distance away from the plane of symmetry. This distance may be calculated using the vector dot product as follows:

$$d_i = (\vec{P}_{\text{sym}} - \vec{n}_i) \cdot \hat{U}_{\text{norm}} \qquad i = 1 \ldots 3 \tag{3.53}$$

where, $\vec{P}_{\text{sym}}$ represents a vector locating any point in the plane of symmetry (n_4, for example). Now, the coordinates of the top plane nodes may be identified as:

$$\vec{n}_{i+6} = \vec{n}_i + (2d_i + L_{jo})\hat{U}_{\text{norm}} \qquad i = 1 \ldots 3 \tag{3.54}$$

where L_{jo} is the length of the midplane joint offset, if any is present.

The forward kinematic procedure now requires only one iterative loop.

3.5.4 Inverse Kinematic Solutions with Symmetry Imposed

This section will discuss two general methods for arriving at a solution to the inverse problem: iterative and closed-form. The ultimate goal of this work is to develop algorithms that will be useful in solving a multi-module manipulator. This section will show that both iterative and closed-form inverse solutions to a single module are possible. The closed-form solution will be utilized in one of the multi-module solution techniques to be discussed later. However, the iterative version

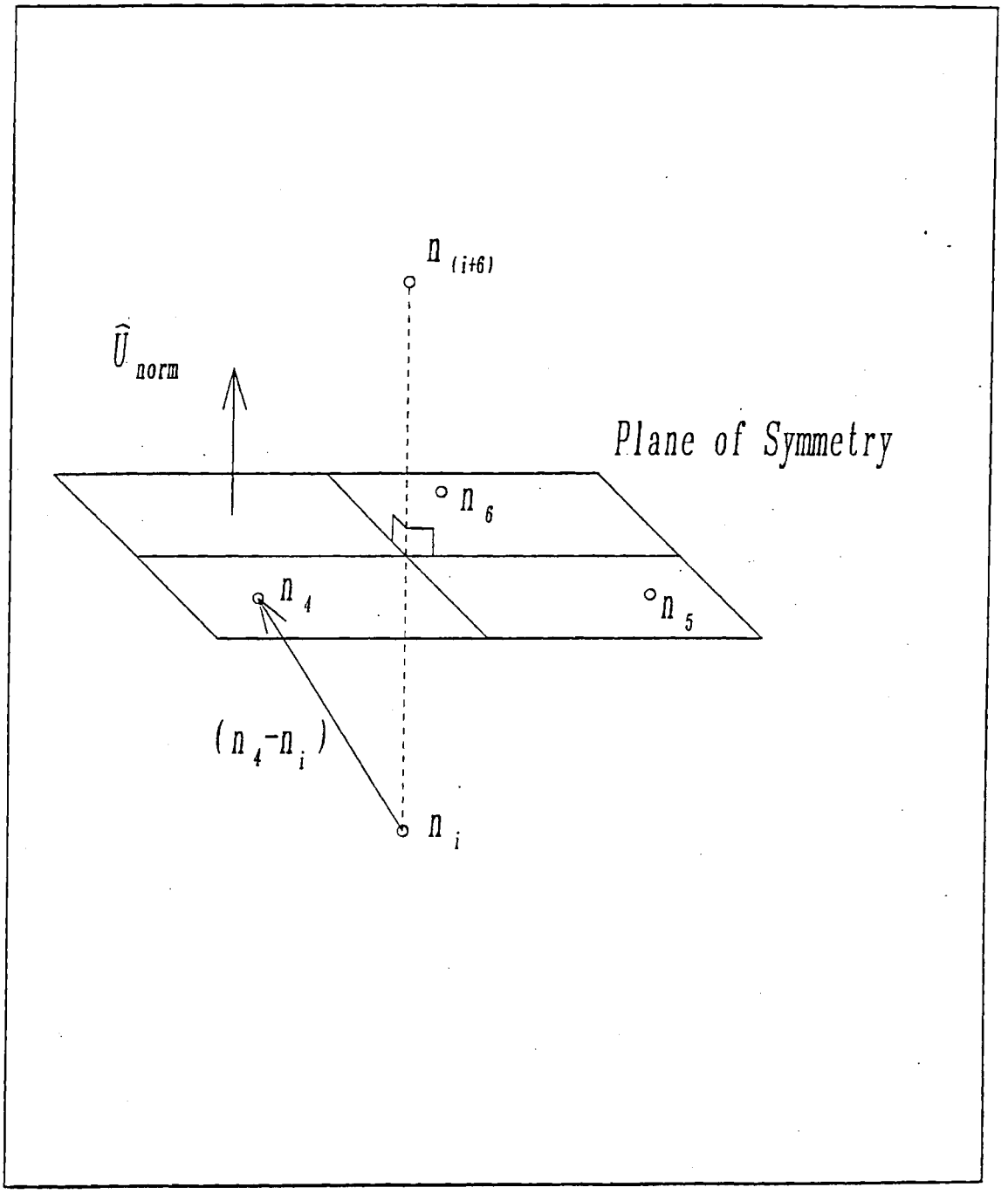

Figure 3.12: Method of projection through the plane of symmetry

provides many insights and will be utilized extensively for other formulations of the multi-module inverse problem.

Iterative Solutions

It was stated earlier that the forward kinematic solution of the symmetric truss requires only one iterative loop. This implies that using the inverse solution outlined for the general double-octahedral geometry will require only four iterative processes per pass, one iteration to determine the present position and orientation given l_1, l_2, and l_3, and three iterations to evaluate the effects of varying l_1, l_2, and l_3. This computational burden can be further reduced. Since the goal of the inverse kinematic problem is to identify the required extensible link lengths, it is not necessary to know the l's until a solution is found. As outlined, the first step in the inverse solution process was to assume values for the l's. This represents the conventional input specification. For this parallel, three DOF device a canonical specification set exists that results in a linear forward solution. If values are assumed for the angles ϕ_1, ϕ_2, and ϕ_3, the positional state of the truss is completely and uniquely defined. The following procedural outline may now be used:

1. Assume a set of ϕ's.
2. Calculate in closed form the midplane nodes.
3. Project the base nodes through the midplane to form the top plane.
4. Compare this to the desired end position. If converged, proceed to step 8.
5. Evaluate the effect of each ϕ on each end parameter (e.g. $\frac{\partial x}{\partial \phi_1}$). These partials may now be evaluated in closed form.
6. Compute a set of $\Delta\phi$'s.
7. Modify the assumed set of ϕ's and return to step 2.
8. Use the final set of ϕ's to compute in closed-form the actual l's required.

The inverse kinematics process now requires just the one main iterative loop. This was accomplished by iteratively solving the closed-form canonical input specification forward kinematic problem.

Closed-Form Solutions

This section summarizes the inverse kinematic research conducted by Padmanabhan, et al.[41, 42], who identified closed-form inverse kinematic solutions for the symmetric, batten-actuated, double-octahedral truss. Since this is a three DOF device, the inverse goal specification can only possess three degrees-of-freedom. For this reason the inverse kinematic problem has been divided into two classes of problems. One class of problems is concerned with identifying the link lengths necessary to produce a given (X, Y, Z) position of the end-effector. This will be termed the inverse positioning problem. The other class of problems is concerned with identifying the link lengths required to produce a given extension and angular

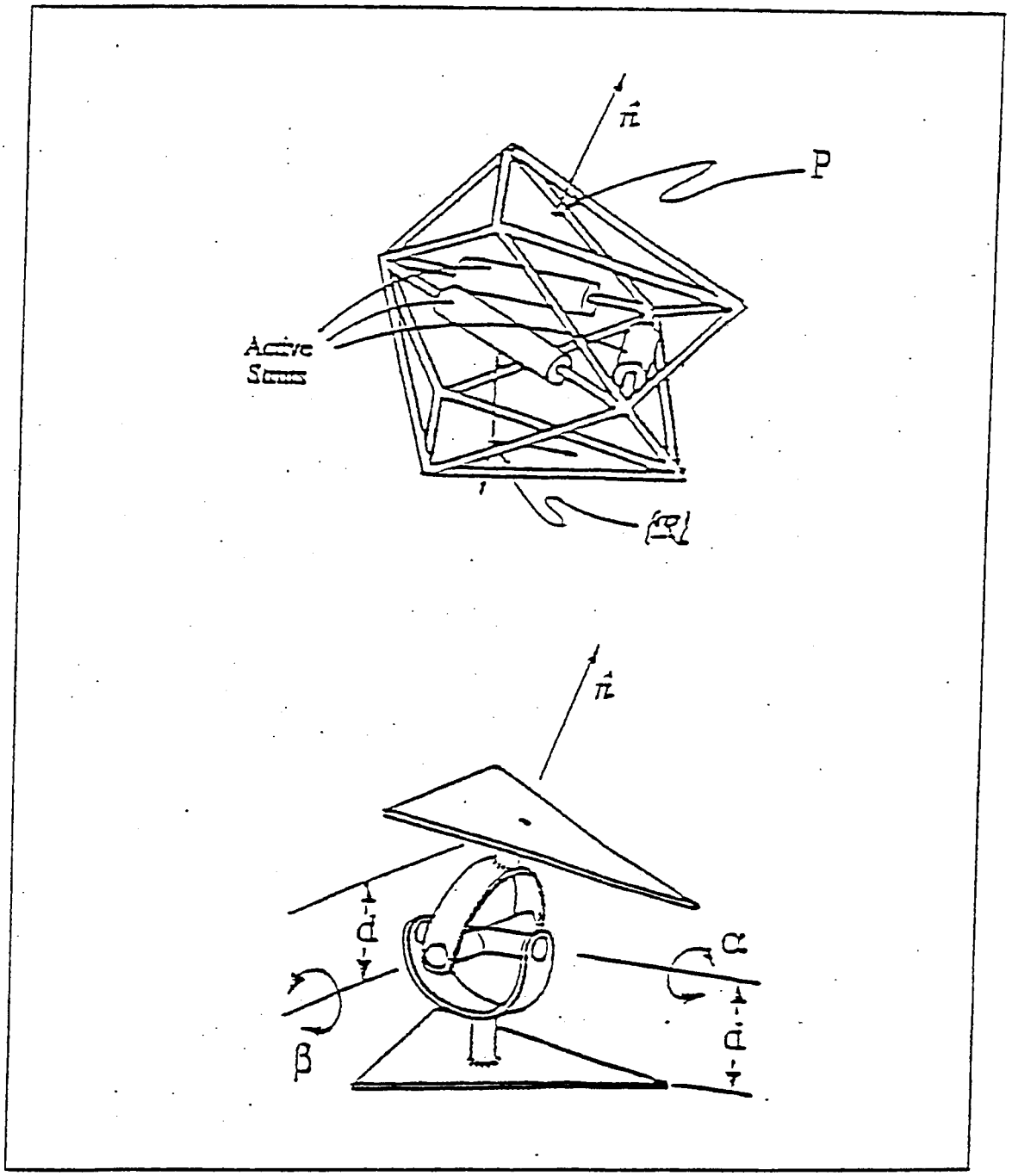

Figure 3.13: Two Possible Goal Specifications for Closed-Form Inverse Analysis

rotation about two axes. This is termed the inverse gimbal problem. Both of theses tasks have been successfully solved in closed form. Figure 3.13 illustrates the two inverse goal concepts. Note that this figure also presents the more intuitive gimbal model of the VGT. This module behaves much like a conventional Hooke's coupling; however, it has the ability to alter the parameter shown as d in Figure 3.13. While these closed-form solutions are extremely useful for solving individual modules, they do not address the problem posed by the modular manipulator where additional DOFs would be chained to the three DOFs module.

3.6 Description of the Static Truss Modules

The static truss sections will be treated in the same manner as the active truss sections. Since there will be no change in geometry of the static sections, a full kinematic analysis is not required. However, each static section must have a known transformation that describes the relative position and orientation of the faces that are designed to accommodate attachment of other truss elements. This transformation can be calculated from the given geometry, or simply measured on the physical truss module. In general, the static sections are in the form of triangular prisms of various lengths and cross-sectional dimensions. A typical assortment of static truss sections is shown in Figure 3.14. Note that some static sections may be tapered and the two end faces may not be parallel. In all cases the critical information to be obtained is the transformation from $\mathcal{B}$ to $\mathcal{T}$.

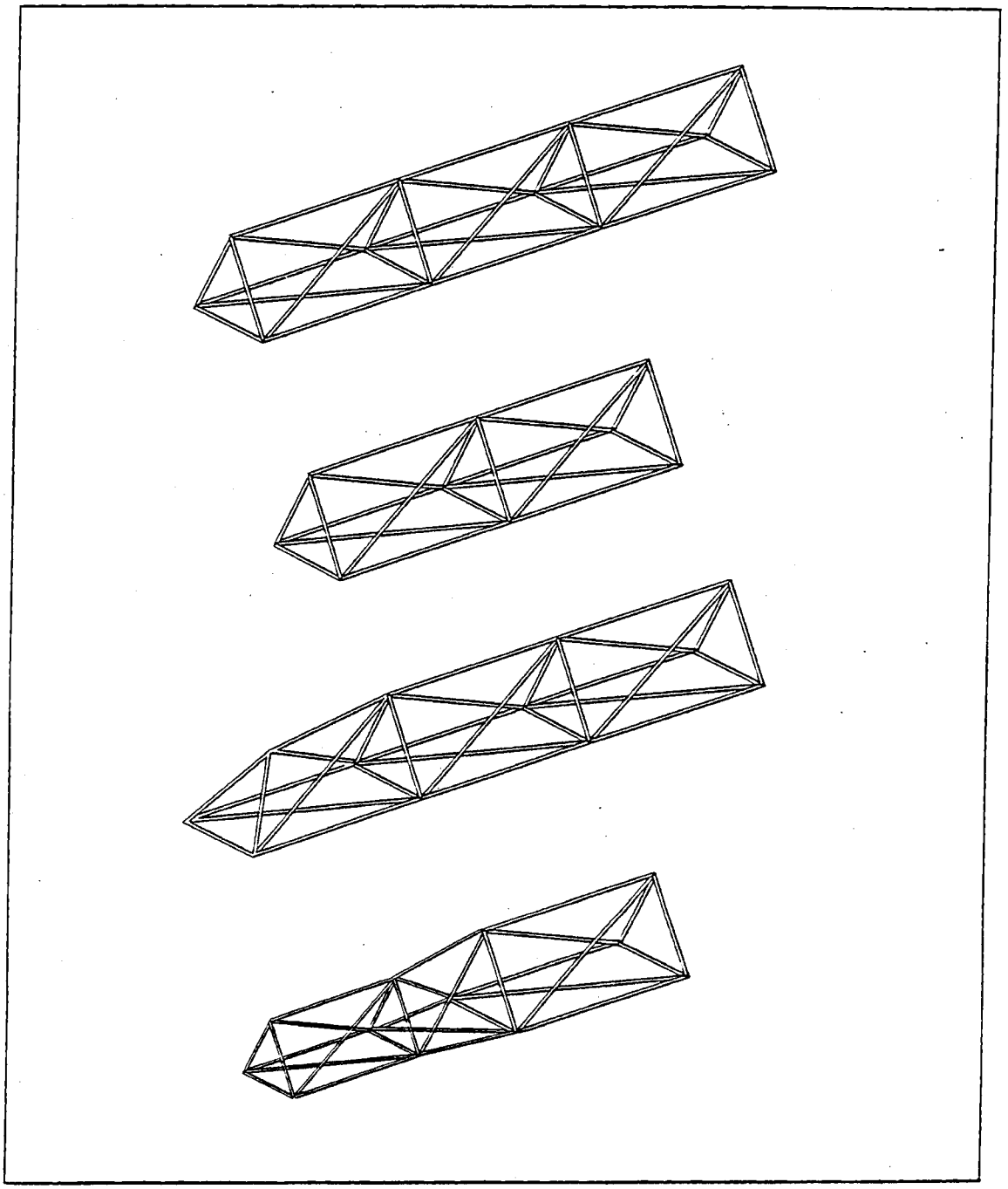

Figure 3.14: Possible Static Truss Sections

4. Conclusion

Truss-based manipulator structures are designed so that the load sustained by each of the links is purely tension or compression. Thus, all of the links are utilized in their strongest loading configuration. The result is an extremely stiff manipulator with a high strength-to-weight ratio. In addition, the modular nature and open framework of the manipulator make the system highly adaptable, rugged and reliable. The open framework is particularly well suited to waste conveyance systems, providing protection for the system while allowing easy access to the entire system.

The kinematics of truss-based manipulators are considerably more complex than those of conventional manipulators. The limited workspace of truss-based manipulator units requires that a truss-based manipulator possess many more degrees of freedom than a conventional manipulator. This further complicates the kinematic analysis.

This report addressed this critical issue in the realization of truss-based manipulators. The kinematics of individual truss-based manipulator units were analyzed in detail, with specific relationships developed for a number of truss structures. These kinematic relationships, either closed-form or with computationally efficient iterative solutions, allow for real-time control of complex, multi-DOF truss-based manipulators.

Bibliography

[1] Arnautovic, S.H., "Adaptive Control of Redundant Manipulators via Pseudovariables," *Proceedings of the IEEE International Conference on Robotics and Automation,*" Cincinnati, OH, May 13-18, 1990.

[2] Arun, V., C.F. Reinholtz, and L.T. Watson, "Application of New Homotopy Techniques to Variable Geometry Trusses," *Transactions of the ASME Journal of Mechanical Design*, Vol. 114, No. 3, Sept. 1992, pp. 422-427.

[3] Arun, V., and C.F. Reinholtz, "Enumeration and Analysis of Variable Geometry Truss Manipulators," *Proceedings of the 1990 ASME Mechanisms Conference*, DE-Vol. 26, Chicago, IL, Sept. 16-19, 1990, pp. 93-98.

[4] Arun, V., B. Padmanabhan, K. Kolady, and C.F. Reinholtz, "Determination of the Workspace of the 3-DOF Double-Octahedral Variable-Geometry Truss Manipulator,"*Proceedings of the 22nd ASME Mechanisms Conference*, DE-Vol. 45, Sept. 1992, pp. 493-500.

[5] Blume, C., et al., "A Combination of Manipulator and Robot for New Out-Door Applications in Unstructured Environments," *Proceedings of the IEEE International Conference on Robotics and Automation*, Piscataway, NJ, May 14-19, 1989, pp. 383-390.

[6] Carignan, C.R., "Trajectory Optimization for Kinematically Redundant Arms," *Journal of Robotic Systems*, Vol. 8, No. 2, 1991, pp. 221-248.

[7] Cheney, W., and D. Kincaid, *Numerical Mathematics and Computing*, Monterey: Brooks/Cole, 1985.

[8] Chirikjian, G.S., and J.W. Burdick, "Kinematics of Hyper-Redundant Manipulators," *Proceedings of the ASME Mechanisms Conference*, Chicago, IL, Sept. 16-19, 1990.

[9] Chirikjian, G.S., and J.W. Burdick, "A Modal Approach to the Kinematics of Hyper-Redundant Manipulators," Robotics and Mechanical Systems Technical Report No. RMS-89-3, CA Inst. of Technology, Sept., 1989.

[10] Clark, W.W., "A Planar Comparison of Actuators for Vibration Control of Flexible Structures," *Proceeding of the 1989 Structures, Structural Dynamics and Materials Conference*, Mobile, AL, April 1989, pp. 1495-1503.

[11] Colbaugh, R., and M. Jamshidi,"Robot Manipulator Control for Hazardous Waste-Handling Applications," *Journal of Robotic Systems*, Vol. 9, No. 2, 1992, pp. 215-250.

[12] Craig, J.J., *Introduction to Robotics, Mechanics and Control*, Reading: Addison-Wesley, 1986.

[13] Dongarra, J.J., C.B. Moler, J.R. Bonch, and G.W. Stewart, *Linpack User's Guide*, SIAM, Philadelphia,PA, 1979.

[14] Dorsey, J.T., "Vibration Characteristics of a Deployable Controllable-Geometry Truss Boom," NASA Technical Paper 2160, June 1983.

[15] Fichter, E.F., " A Stewart Platform-Based Manipulator: General Theory and Practical Construction," *The International Journal of Robotic Research*, Vol. 5, No. 2, Summer 1985.

[16] Golub, H., and C.F. Van Loan, *Matrix Computations*, Baltimore: Johns Hopkins UP, 1983.

[17] Griffis, M., and J. Duffy, "A Forward Displacement Analysis od a Class of Stewart Platforms," Gainsville: Center for Intelligent Machines and Robotics, Jan. 1989.

[18] Hollerbach, "Optimum Kinematic Design for a Seven Degree of Freedom Manipulator," *Proceedings from Robotics Research - The Second International Symposium*, Cambridge, MA, pp. 216-222.

[19] Hunt, K.H., "Structural Kinematics of In-Parallel-Actuated Robot Arms," *Transactions of the ASME Journal of Mechanisms, Transmissions, and Automation in Design*, Vol. 105, 1983, pp. 705-712.

[20] Jain, S., and S. Kramer, "Design of a Variable Geometry Robot Based on an n-Celled Tetrahedron-Tetrahedron Truss," *Proceedings of the 1988 ASME Design Technology Conference*, Kissimmee, FL, DE Vol. 15-3, 1988, pp. 119-123.

[21] Kahanar, D., et al., *Numerical Methods and Software*, Englewood Cliffs: Prentice Hall, 1989.

[22] Kelmar, L., and P.K. Khosla, "Automatic Generation of Forward and Inverse Kinematics for a Reconfigurable Modular Manipulator System," *Journal of Robotic Systems*, Vol. 7, No. 4, 1990, pp. 599-620.

[23] Kelmar, L., and P.K. Khosla, "Automatic Generation of Kinematics for a Reconfigurable Modular Manipulator System," *Proceedings of IEEE International Conference on Robotics Automation*, Philadelphia, PA, Vol. 2, 1988, pp. 663-668.

[24] Krieg, S.A., et al., *Single-Shell Tank Waste Retrieval Study*, Prepared for U.S. D.O.E. Office of Environmental Restoration and Waste Management, Richland: Westinghouse Hanford Co., June 1990.

[25] Lee, K.M., and A. Chao, "On the Analysis of a Three-Degrees-of-Freedom Manipulator," *The International Journal of Robotics and Automation*, Vol. 3, No. 2, 1988, pp. 90-96.

[26] Lossing, D.L., and A.L. Eshleman, "Planning a Common Database for Engineering and Manufacturing," *Proceedings of the SHARE XLIII Conference*, Chicago, IL, Aug. 1974.

[27] Mabie, H., and C.F. Reinholtz, *Mechanisms and Dynamics of Machinery*, New York: J. Wiley and Sons, 1987.

[28] Maciejewski, A.A., "Real-Time SVD for the Control of Redundant Robotic Manipulators," *Proceedings of the IEEE International Conference on Systems Engineering*, Fairborn, OH, Aug. 24-26, 1989, pp. 549-552.

[29] Mayorga, R.V., and A.K.C. Wong, "A Global Approach for the Optimal Path Generation of Redundant Robot Manipulators," *Journal of Robotic Systems*, Vol. 7, No. 1, 1990, pp. 107-128.

[30] Miura, K., H. Furuya, and K. Suzuki, "Variable Geometry Truss and its Application to Deployable Truss and Space Crane Arm," *Proceedings from the 35th Congress of the International Astronautical Federation*, Lausanne, Switz., Oct. 1984.

[31] Miura, K., and H. Furuya, "An Adaptive Structure Concept for Future Space Applications," *Proceedings from the 36th Congress of the International Astronautical Federation*, Stockholm, Swed., Oct. 1985.

[32] Mortenson, M.E., *Geometric Modeling*, New York: J. Wiley and Sons, 1985.

[33] Naccarato, F. and P.C. Hughes, "Inverse Kinematics of Variable-Geometry Truss Manipulators," *Journal of Robotic Systems*, Vol. 8, No. 2., 1991, pp. 249-266.

[34] Nakamura, Y., *Advanced Robotics: Redundancy and Optimization*, Reading: Addison-Wesley, 1991.

[35] Natori, M., K. Iwasaki, and F. Kuwao, "Adaptive Planar Truss Structures and Their Vibration Characteristics," *Proceedings of the 1987 Structures, Structural Dynamics and Materials Conference*, Monterey, CA, April 1987, pp. 143-151.

[36] Nayfeh, A. H., "Kinematics of Foldable Discrete Space Cranes," publication of the Department of Aerospace Engineering and Engineering Mechanics, Cincinnati: U of Cincinnati, 1985.

[37] Nikravesh, P.E., *Computer Aided Analysis of Mechanical Systems*, Englewood Cliffs: Prentice Hall, 1988.

[38] Noble, B., *Applied Linear Algebra*, Englewood Cliffs: Prentice Hall, Inc., 1969.

[39] Oh, S., "Inverse Kinematic Control for Redundant Manipulators," *Proceedings of the IEEE Workshop on Intelligent Control*, Troy, NY, Aug. 26, 1985, pp. 53-57.

[40] Padmanabhan, B., "Design of Robotic Manipulators Using Variable Geometry Trusses as Joints," *Proceedings of the First National Applied Mechanisms and Robotics Conference*, Vol. 11, 1989, paper 89 AMR-8C-7.

[41] Padmanabhan, B., V. Arun, and C.F. Reinholtz, "Closed-Form Inverse Kinematic Analysis of Variable Geometry Truss Manipulators, " *Transaction of the ASME Journal of Mechanical Design*, Vol 114, No. 3, Sept. 1992, pp. 438-443.

[42] Padmanabhan, B., P.H. Tidwell, R.J. Salerno, and C.F. Reinholtz, "VGT-Based Gimbals: Practical Construction and General Theory," *Proceedings of the 22nd ASME Mechanisms Conference*, DE-VOL 46, Sept. 1992, pp. 437-443.

[43] *PC-MATLAB for MS-DOS Personal Computers*, South Natick: The MathWorks, Inc., 1989.

[44] Press, W.H., et al., *Numerical Recipes in C*, New York: Cambridge UP, 1988.

[45] Reinholtz, C.F., and D. Gokhale, "Design and Analysis of Variable Geometry Truss Robots," *Proceedings of the 10th Applied Mechanisms Conference*, New Orleans, LA, Dec. 6-9, 1987.

[46] Rhodes, M.D., and M.M. Mikulas Jr., "Deployable Controllable Truss Beam," NASA Technical Memorandum 86366, June 1985.

[47] Robertshaw, H.H., and C.F. Reinholtz, "Variable Geometry Trusses," *Proceedings of the US Army Research Office Workshop on Smart Materials, Structures and Mathematical Issues*, Sept. 15-16, 1988.

[48] Salerno, R.J., *Shape Control of High Degree-of-Freedom Variable Geometry Truss Manipulator*, Thesis, Virginia Polytechnic Inst. and State U, Blacksburg: VPI & SU, 1989.

[49] Salerno, R.J., C.F. Reinholtz, and H.H. Robertshaw, "Shape Control of High Degree of Freedom Variable Geometry Trusses," *Proceedings of the NASA Workshop on Controls/Structures Interaction*, Williamsburg, VA, July 11-13, 1988.

[50] Salerno, R.J., C.F. Reinholtz, and S.G. Dhande, "Kinematics of Long-Chain Variable Geometry Truss Manipulators," *Advances in Robot Kinematics*, Eds. S. Stifter and J. Lenarcic, Vienna, Aus.: Springer-Verlag, 1991, pp. 179-187.

[51] Salerno, R.J., H.H. Robertshaw, C.G. Horner, W.J. Milsap, D.W. Bennett, "Proposed use of a Variable Geometry Truss Manipulator for Radioactive

Waste Removal from Underground Stroage Tanks," *Proceedings of the 1992 Waste Management Conference*," Tucson, AZ, March 1992.

[52] Sincarsin, W.G., "Trussarm Conceptual Design," Dynacon Report 28-611/0402, April 1987.

[53] Sincarsin, W.G., and P.C. Hughes, "Trussarm Candidate Geometries," Dynacon Report 28-611/0401, April 1987.

[54] Sklar, M., and D. Tesar, "Dynamic Analysis of Hybrid Serial Manipulator Systems Containing Parallel Modules," *Transactions of the ASME Journal of Mechanisms, Transmissions, and Automation in Design*, Vol. 105, No. 2, June 1988, pp. 109-115.

[55] *Spar Aerospace Limited Applies Advanced Technology to Environmental Restoration Projects*, Brampton, Ontario: Spar Aerospace Limited, [1992?].

[56] Stewart, D., "A Platform with Six Degrees of Freedom," *Proceedings of the Institute of Mechanical Engineers*, Vol. 180, Part 1, No. 15, 1965-1966, pp. 371-386.

[57] Stoer, J., and R. Bulirsch, *Introduction to Numerical Analysis*, Trans. R. Bartel, et al., New York: Springer-Verlag, 1993.

[58] Sugimoto, K., "Kinematic and Dynamic Analysis of Parallel Manipulators by Means of Motor Algebra," *Transactions of the ASME Journal of Mechanisms, Transmissions, and Automation in Design*, Vol. 109, No. 1, Mar. 1987, pp. 3-7.

[59] Sugimoto, K., "Computational Scheme for Dynamic Analysis of Parallel Manipulators," *Transactions of the ASME Journal of Mechanisms, Transmissions, and Automation in Design*, Vol. 111, No. 1, Mar. 1989, pp. 29-33.

[60] Suh, K.C., and J.M. Hollerbach, "Local versus Global Torque Optimization of Redundant Manipulators," *Proceedings of the IEEE International Conference on Robotics and Automation*, Raleigh, NC, March 31 - April 3, Vol. 2, 1987, pp. 619-624.

[61] Tesar, D., and D.J. Cox, "The Dynamic Modeling and Command Signal Formulation for Parallel Multi-Parameter Robotic Devices," Gainsville: Center for Intelligent Machines and Robotics, 1981.

[62] Tidwell, P.H., "Design and Construction of a Double-Octahedral Variable Geometry Truss Manipulator," Master's Thesis, Virginia Polytechnic Inst. and State U, Blacksburg: VPI & SU, July 1989.

[63] Tidwell, P.H., C.F. Reinholtz, H.H. Robertshaw, and C.G. Horner, "Kinematic Analysis of Generalized Adaptive Trusses," *Proceedings of the First Joint US/Japan Conference on Adaptive Structures*, Maui, Hawaii, Nov. 13-15, 1990.

[64] Wynn, R.H. Jr., H.H. Robertshaw, and C.G. Horner, "An Analytical Study of a Six Degree of Freedom Active Truss for use in Vibration Control," Proceeding of the AIAA Structures, Structural Dynamics, and Materials Conference, Long Beach, CA, April 1990, AIAA Paper 90-1164-CD.

[65] Yang, D.C., and T.W. Lee, "Feasibility Study of a Platform Type of Robotic Manipulator from a Kinematic Viewpoint," *Transactions of the ASME Journal of Mechanisms, Transmissions, and Automation in Design*, Vol. 106, June 1984, pp. 191-198.

[66] *Environmental Restoration and Waste Management Robotics Technology Development Program, Robotics Five-Year Plan*, DOE/CE-0007T, Vol. 1-3, United States Department of Energy, Washington D.C., 1990.